Renewable and Sustainable Energy Reviews 13 (2009) 1734–1759

Contents lists available at ScienceDirect

Renewable and Sustainable Energy Reviews

journal homepage: www.elsevier.com/locate/rser

A review of the mathematical models for predicting solar air heaters systems

Réné Tchinda [a,b,*]

[a] IUT FOTSO VICTOR, University of Dschang, PO Box 134 Bandjoun, Cameroon
[b] ICTP Strada Costiera 11, 34014 Trieste, Italy

ARTICLE INFO

Article history:
Received 29 September 2008
Accepted 14 January 2009

Keywords:
Solar air heater collectors
Mathematical model
Designs
Energy balance equations
Exergy analysis

ABSTRACT

A mathematical model of the closed solar air heaters is used in particular, to assist in interpreting the observed phenomena in the solar air heaters, to design the system, to predict the trends, and to assist in optimization. In this paper, various mathematical models, mainly analyzing the heat transfer process of solar air heaters, are reviewed and classified based on the model, the number of the cover, the shape of the absorber and the presence or not of the packing bed. Although the models have evolved to a point where several features of the process can be predicted, more effort is required before the models can be applied to define actual operating conditions as well as to further investigate new closed solar air heaters. It is shown that the major governing equations in the models are based on the first law of thermodynamics.

Contents

* Correspondence address: IUT FOTSO VICTOR, University of Dschang, PO Box 134, Bandjoun, Cameroon. Fax: +237 33014601.
E-mail address: ttchinda@yahoo.fr.

1364-0321/$ – see front matter © 2009 Elsevier Ltd. All rights reserved.
doi:10.1016/j.rser.2009.01.008

1. Introduction

One of the most potential applications of solar energy is the supply of hot air for the drying of agricultural, textile and marine products, and heating of buildings to maintain a comfortable environment especially in the winter season. Several designs for solar air heaters have been proposed and discussed in literature. The designer and potential user of these systems must consider a number of factors when comparing their merits. These can mainly be categorized as: (i) thermal performance, (ii) cost and (iii) lifetime, durability, maintenance and ease of installation. Thermal performance of collectors is compared by using the concept of thermal efficiency. It is generally believed that the thermal efficiency of a solar collector is the major requirement for the prediction of thermal performance of the complete solar system of which the solar air collector is a part [1]. It is, therefore, important that this thermal efficiency information be in a form which is useful for existing and projected future solar energy system design methods. To save energy, the method of exergy analysis is useful in solar systems, because it appears to be an essential tool for system design, analysis and optimization of thermal systems [2]. One indication is that there are about two review papers in the area of solar air heaters published in recent years. The first was proposed by Chandra and Sodha [1]. These authors have provided a fundamental understanding of testing procedures for solar air heaters. The second was proposed by Ekechukwu and Norton [3]. They have classified solar air heaters broadly into two types: bare plate and cover plate solar energy collectors. Based on this classification, these authors have summarized various designs of solar air heaters.

With the development of computer, hardware and numerical methodology, advanced mathematical models are being used to carry out critical investigations on solar air heaters. The advantages of these methods are that they can produce extremely large volumes of results at virtually no added expense and it is very cheap to perform parametric studies to optimize equipment performance. The second reason for such work on numerical simulation is that some parameters are difficult to test, and experimental study is expensive as well as time consuming.

The purpose of this work is to review the present state of mathematical modeling of solar air heaters. The validation is an important step in mathematical modeling development, and therefore comparisons with actual experimental values or theoretical results have been included where possible. Since most of the models have to be solved numerically, the numerical techniques employed in the solution of different models are presented.

Nomenclature

A	area element
B	height of solar air collector
C	specific heat
D	depth of air channel
Dh	equivalent diameter of air channel
h	heat transfer coefficient
k	thermal conductivity
L	Length of air heater
M	mass per unit collector area
m	mass flow rate
Nu	Nusselt number
Pr	Prandtl number
R	recycle ratio
r	fraction of the mass flow rate
Ra	Rayleigh number
Re	Reynolds number
S	incident solar radiation
T	temperature
t	time
U	loss coefficient
V	wind speed
W	width of absorber (collector width)
x,y	space coordinate
Greek letters	
α	solar absorbance
δ	thickness
ε	emissivity
σ	Stefan–Boltzmann constant
τ	Transmitivity
ρ	reflectance
ρ_f	fluid density
Subscript	
a	ambient
b	bottom plate
c	convection
f	fluid (air)
g	cover
i	inlet
o	outlet
p	absorber plate
r	radiatif
T,t	top

2. Mathematical models

2.1. A bare plate solar air heater

This consists of a single channel design with single air flow between absorber and bottom plates with insulation (see Fig. 1). Choudhury et al. [4] studied the thermal performance of this model. The energy balance equations for the absorber plate and the rear plate have been written as

$$\text{Bare plate}: \quad \alpha_p S = h_{pa}(T_p - T_a) + h_{pb}(T_p - T_b) + h_{pf}(T_p - T_f) \tag{1}$$

$$\text{Rear plate}: \quad h_{pb}(T_p - T_b) = h_{bf}(T_b - T_f) + U_b(T_b - T_a) \tag{2}$$

With a design selection methodology whereby, for combined fixed values of pressure drop, air-flow rate and duct length, duct-depth values and the resultant values of forced convective heat-transfer

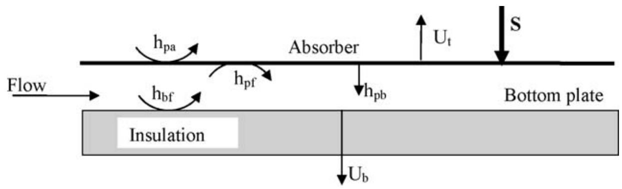


Fig. 1. A schematic view of a bare plate solar air heater [4,7–9].

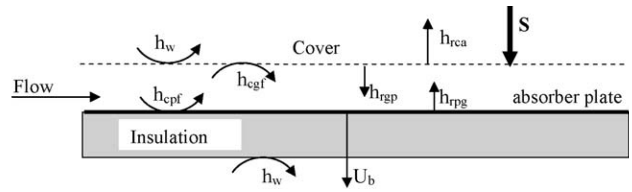


Fig. 2. A schematic view of a single cover solar air heater [7,9,13,16].

coefficients, air-temperature increment per unit incident flux and system efficiency have been computed. From the discussion, it was shown that the computation methodology and the design curves obtained can be successfully used to construct solar air heaters with pre-determined acceptable values of pressure drop with the required rate of air flow, minimum material cost and highest possible efficiency.

Thermal performance of this design has also been predicted by Ong [7]. The mathematical model proposed by this author is similar to the one of Choudhury et al. [4] with a small change in Eq. (1) where, h_{pa} is replaced by $U_b = h_w + h_{rgs}$. In this mathematical model, the solar collector was assumed sufficiently short for which the assumptions were valid. The mathematical solution procedure involved a matrix inversion of the mean temperature vector derived from energy equations. Predicted temperatures for the solar air heaters were presented. The effects of wind and film heat transfer coefficients on the prediction were discussed.

Njomo [8] and Njomo and Daguenet [9] have investigated heat transfer in the above design (Fig. 1). With general assumptions in the heat transfer modeling, the energy balance equations of different components of the solar air heater have been written as:

$$\text{For selective absorber}: \quad M_p C_{pp}\frac{dT_p}{dt} = \alpha_p S - h_{rpb}(T_p - T_b) - h_{cpf}(T_p - T_f) - (h_{cpa} + h_{rpa})(T_p - T_a) \tag{3}$$

$$\text{For air flow}: \quad \rho_f e_f C_{pf}\frac{\partial T_p}{\partial t} + \frac{m_f C_{pf}}{W}\frac{\partial T_p}{\partial x} = h_{cpf}(T_p - T_f) + h_{cbf}(T_b - T_f) \tag{4}$$

$$\text{For bottom plate}: \quad M_b C_{pb}\frac{dT_b}{dt} = h_{rpb}(T_p - T_b) - h_{cbf}(T_b - T_f) - U_b(T_b - T_a) \tag{5}$$

With the mathematical model proposed, Njomo [8] predicted the thermal performance of such a collector. To determine a solar air heater thermal behavior, Njomo and Daguenet [9] used a sensitivity analysis which is an excellent technique to help designers and decision makers in anticipating and preparing for a solar system project. The results have demonstrated the existence of an important dimensionless parameter referred to as thermal performance factor of the collector that compares the useful energy that can be extracted from the heater to its overall heat losses. A detailed sensitivity analysis has been performed, and the results successfully summarized to measure the impact of changes in operation and meteorological parameters on the simulation values of the thermal efficiency and the fluid temperature rise between entrance and exit of the heater.

2.2. Single one cover solar air heater

This design consists of single channel with single air flow between the cover and absorber plate (see Fig. 2). Many authors have investigated the thermal performance of this design [7,9,13–18].

Garg et al. [13] developed the transient heat transfer model of a single one cover solar air heater. This transient model has included the thermal capacitance effects and the conduction losses. The energy balance for each component of the collector yields the following:

$$\text{Cover glass}: \quad \alpha_g S = M_g C_g\frac{\partial T_g}{\partial t} + k_g\delta_g\frac{\partial^2 T_g}{\partial x^2} + h_w(T_g - T_a) + h_{rgs}(T_g - T_s) + h_{cgf}(T_g - T_f) + h_{rpg}(T_g - T_p) \tag{6}$$

$$\text{Absorber plate}: \quad \alpha_p\tau_p S = M_p C_p\frac{\partial T_p}{\partial t} + k_p\delta_p\frac{\partial^2 T_p}{\partial x^2} + h_{cpf}(T_p - T_f) + h_{rpg}(T_p - T_g) + U_r(T_p - T_a) \tag{7}$$

$$\text{Air flow}: \quad M_f C_f\frac{\partial T_f}{\partial t} + \frac{G_f C_f}{W}\frac{\partial^2 T_f}{\partial x^2} = h_{cgf}(T_f - T_g) + h_{cpf}(T_p - T_f) \tag{8}$$

The solar radiation data and ambient temperature have been represented by Fourier series as follows:

$$S = 237.17 + 388.7\cos(t\omega_1 - 3.272) + 195.8\cos(2t\omega_1 - 0.2757) + 27.62\cos(3t\omega_1 - 3.8) + 38.44\cos(4t\omega_1 - 3.44) + 17.76\cos(5t\omega_1 - 4.536) \tag{9}$$

and

$$T_a = 14.354 + 6.11\cos(t\omega_1 - 3.858) + 1.88\cos(2t\omega_1 - 0.509) + 0.225\cos(3t\omega_1 - 1.25) + 0.288\cos(4t\omega_1 - 2.62) + 0.146\cos(5t\omega_1 - 3.92) \tag{10}$$

with $\omega_1 = (\pi/12)$ rd/h.

The initial conditions considered by these authors were: $T_f(t=0) = T_p(t=0) = T_g(t=0) = T_a(t=0)$ and the boundary conditions were given as follow:

$$\left.\frac{\partial T_g}{\partial x}\right|_{x=0} = 0, \quad \left.\frac{\partial T_g}{\partial x}\right|_{x=L} = 0, \quad \left.\frac{\partial T_p}{\partial x}\right|_{x=0} = 0, \quad \left.\frac{\partial T_p}{\partial x}\right|_{x=L} = 0, \tag{11}$$

Eqs. (6)–(8) have been solved numerically using explicit finite difference analysis. The results showed the effect of various design parameters of the heater on its performance.

This design of solar air heater has also been investigated by Ong [7]. Using the thermal network, the following equations have been written for a single one cover solar air heater [7]:

$$\text{Cover}: \quad \alpha_g S + h_{rpg}(T_p - T_g) + h_{cgf}(T_f - T_g) = (h_w + h_{rs})(T_g - T_a) \tag{12}$$

The wind heat transfer h_w has been computed using (A1):

$$\text{Fluid between cover and absorber}: \quad h_{cpf}(T_p - T_f) = h_{cgf}(T_f - T_g) + 2mc_p\frac{(T_{fm} - T_{fi})}{WL} \tag{13a}$$

with

$$T_{fm} = \frac{(T_{fo} + T_{fi})}{2} \tag{13b}$$

$$\text{Absorber plate}: \quad \tau_g \alpha_p S = h_{cpf}(T_p - T_f) + h_{rpg}(T_p - T_g) + U_b(T_p - T_a) \tag{14}$$

The methodology used for this design of solar air heater is similar to the one used by the authors to study a bare plate solar heater.

The mathematical model proposed by Naphon and Kongtragool [17] is similar to the one of Ong [7] instead of Eq. (14) which is replaced by

$$mC_p \frac{dT_f}{dx} = h_{fg}(T_f - T_g) + h_{fp}(T_p - T_f) \tag{15}$$

The above equations proposed by Naphon and Kongtragool [17] have been solved by the explicit method of the finite difference scheme. The results obtained from the model have been compared with the experimental data of Yeh et al. [25]. It appeared that numerical results and experimental data are in good agreement.

Mohamad [15] investigated also this design of solar air heater. The equations proposed by this author are similar to those of Naphon and Kongtragool [17], instead of equation for the cover which did not contain the term of radiative exchange between the glass cover and an ambient. The main objective of this author was to minimize heat losses from the front cover of the collector and to maximize heat extraction from the absorber.

With the aim to determine the flow channel optimum geometry of this single cover solar air heater (Fig. 2), Hegazy [16] proposed a new mathematical model. This model was based on the following assumptions: (i) the flow channel was hydraulically smooth; (ii) there was no air leakage to or from the heater; (iii) heat capacity effects of glass cover, enclosed air, absorber and bottom plate were negligible; (iv) the temperatures of glass, absorber and bottom plates were varied only along the *x*-direction of the air flow; and (v) the solar air heater consisted of a number elements so that the temperatures of the element surfaces are uniform, while that of the air stream inside varies linearly along its small length. With these assumptions, the energy balance equations have been written as

$$\text{For glass cover}: \quad \alpha_g S + h_{rpg}(T_p - T_g) + h_{cgf}(T_{fm} - T_g) = (h_w + h_{rs})(T_g - T_a) \tag{16}$$

where T_{fm} is given by Eq. (13b).

For air stream between cover and absorber

$$: \quad h_{cpf}(T_p - T_{fm}) = h_{cgf}(T_{fm} - T_g) + 2GC_p \frac{(T_{fm} - T_{fi})}{L/dx} \tag{17}$$

G is a specific mass rate.

$$\text{At absorber plate}: \quad \tau_g \alpha_p S = h_{cpf}(T_p - T_{fm}) + h_{rpg}(T_p - T_g) + U_b(T_p - T_a) \tag{18}$$

An iterative procedure has been employed by the author to analyze the performance of this solar air heater in terms of useful energy, thermal efficiency and air temperature rise.

Hegazy [26] investigated the effect of variation in the absorber width on both the thermal and hydraulic performances of a single cover solar air heater (Fig. 2). In addition to the assumption made by the author [16], it was assumed that heat transfer is quasi-steady and one dimensional, and that turbulent air flow inside small element temperatures varies linearly along its small length. Hence, the energy balance equations of this design of solar air collector are given by Eqs. (16) and (18) for glass cover and absorber plate. For the air stream, the energy equation has written as

$$h_{cpf}(T_p - T_{fm})Wdx = h_{cgf}(T_{fm} - T_g)Wdx + mC_p(T_{fo} - T_{fi}) \tag{19}$$

U_b has been computed using the same equation as Hegazy [16], in which $W = \overline{W}(x)$ is the average width of an element dx at a distance x from the inlet and $G = m/A_p$. This study was considered as a more general and fundamental case when variable width absorbers were utilized, instead of conventional rectangular plates, in collecting incident solar radiation. The results indicated the variable width collectors with shape parameters exhibit performance behavior.

Aboul-Enein et al. [27] have analyzed this solar air heater device with and without thermal storage. In order to write the energy balance equations, these authors have made the following assumptions: (i) the heat capacities of the glass cover, absorbing plate and insulation were negligible; (ii) there was no temperature gradient across the thickness of the glass cover and the storage material has an average temperature at time *t*. (iii) the system was perfectly insulated and there was no air leakage from the collector; (iv) no stratification existed perpendicular to the air flow. Without the storage material, the energy balance equations of the glass cover and for the plate are similar to those proposed in the mathematical model of Hegazy [16]. For the air flow, the model was written as

$$h_{cpf}(T_p - T_f)W = mC_f \frac{\partial T_f}{\partial x} + d_f \rho_f W C_f \frac{\partial T_f}{\partial t} + h_{cfg}(T_f - T_g)W + U_t(T_f - T_a)W \tag{20}$$

with the storage material, the energy balance equation for the glass cover has the same form as without the storage material. However, the energy balance equations for the absorber plate and storage material were written as follow:

$$\text{For the absorber plate}: \quad \tau_g \alpha_p S = h_{rpg}(T_{ps} - T_{gs}) + h_{cpf}(T_{ps} - T_{fs}) + \frac{k_p}{z_p}(T_{ps} - T_{st}) \tag{21}$$

$$\text{For the storage material}: \quad \frac{k_p}{z_p}(T_{ps} - T_{st})A_p = M_{st}C_{st}\frac{dT_{st}}{dt} + U_b(A_b + A_s)(T_{st} - T_a) \tag{22}$$

The forced convective heat h_{cga} is given in Appendix A.

A computer program was prepared for the solution of this mathematical model. An optimization process for a flat plate solar air heater with and without thermal storage was carried out. Comparisons between experimental and theoretical results indicated that the proposed mathematical model could be used for estimating the thermal performance of flat plate solar air heaters with reasonable accuracy.

Zhai et al. [18] have recently investigated a single cover solar air heater integrated with the building. Based on some assumptions, the equations governing the performance of the solar air heater were given by equations similar to (12)–(14) without the term of the radiative exchange between cover and the sky, and with $Q_1 = mC_p(T_{fo} - T_r)$ and $U_b = [1/h_{cbattic} + \delta_b/k_b]^{-1}$.

Njomo [14] and Njomo and Daguenet [9] analyzed the heat transfer in the single cover solar air heater. The following energy balance equations have been written for the components of this design:

For combined plastic–glass transparent cover:

$$M_g C_{pg} \frac{dT_g}{dt} = \alpha_g S + h_{rpg}(T_p - T_g) + h_{cgf}(T_f - T_g) - (h_{cga} + h_{rca})(T_g - T_a) \tag{23}$$

$$\text{For air flow}: \quad \rho_f e_f C_{pf}\frac{\partial T_p}{\partial t}+\frac{mC_{pf}}{W}\frac{\partial T_p}{\partial t} = h_{cpf}(T_p - T_f) - h_{cgf}(T_f - T_g) \quad (24)$$

$$\text{For absorber plate}: \quad M_p C_{pp}\frac{dT_p}{dt} = (\alpha\tau)S - h_{cpf}(T_p - T_f) - h_{rpg}(T_p - T_g) - (U_b + h_{rpa})(T_p - T_a) \quad (25)$$

The optical efficiency of the collector is given by [29]:

$$(\tau\alpha) = \frac{\tau_g \alpha_p}{1-(1-\alpha_p)\rho_g} \quad (26)$$

T_{sky} was given by the correlation proposed by Clark [12]. This mathematical model has been used by Njomo [30] to study the cost of the energy extracted from these collectors as a function of their lifetime. Numerical calculations have been performed for glass cover and plastic cover air collectors of the same dimensions under identical conditions of insolation and mass flow rate. The results showed that a significant gap exists between the thermal performances of the glass cover and plastic cover air collectors and the useful energy delivered by the plastic cover air collector is cheaper than the energy extracted from the glass cover air collector.

2.3. Single two covers solar air heater

This collector is made of two covers and a single channel air flow between the second cover and absorber plate, and insulation (Fig. 3). This model has been studied by Njomo and Daguenet [9], Mohamad [15], Naphon and Kongtragool [17] and Njomo [31].

Mohamad [15] investigated heat transfer in this design. Under steady state operating conditions, the energy balances equations for the mentioned collector written by this author are

$$\text{For the top cover}: \quad \alpha_{g1}S = h_w(T_{g1} - T_a) + h_{cg1g2}(T_{g1} - T_{g2}) + h_{rg1g2}(T_{g1} - T_{g2}) \quad (27)$$

$$\text{For second glass cover}: \quad \alpha_{g2}\tau_{g1}S = h_{cg2f}(T_{g2} - T_f) + h_{cg1g2}(T_{g2} - T_{g1}) + h_{rg1g2}(T_{g2} - T_{g1}) + h_{rg2p}(T_{g2} - T_p) \quad (28)$$

$$\text{For air stream}: \quad mC_p\frac{dT_f}{dx} = h_{cg2f}(T_{g2} - T_f) + h_{cpf}(T_p - T_f) \quad (29)$$

$$\text{For absorber plate}: \quad \alpha_p\tau_{g1}\tau_{g2}S = h_{cpf}(T_p - T_f) + h_{rpg2}(T_p - T_{g2}) + U_b(T_p - T_a) \quad (30)$$

Naphon and Kongtragool [17] have studied this design. The mathematical model obtained by these authors is similar to the model of Mohamad [15] with change in the equation describing the heat transfer in the upper cover in which the radiative exchange between the upper cover and ambient is taken into account.

Njomo and Daguenet [9] and Njomo [31] have also investigated heat transfer in this design (with plexigas–glass cover, glass cover-glass cover and plastique-vitre). These authors in their investigation have considered the two covers as a combined system which is characterized by one heat transfer equation. In this case the energy balance equations of the different component of the solar air heater design are given by Eqs. (23)–(25) without the radiative exchange between absorber plate and sky. $(\tau\alpha)$ is given by Eq. (26) with:

$$\tau_g = \frac{\tau_{g1}\tau_{g2}}{1-\rho_{g1}\rho_{g2}} \quad (31a)$$

$$\rho_g = \rho_{g1} + \frac{\rho_{g2}\tau_{g1}^2}{1-\rho_{g1}\rho_{g2}} \quad (31b)$$

$$\alpha_g = 1 - \rho_g - \tau_g \quad (31c)$$

In the mathematical model studied by Njomo and Daguenet [9] and Njomo [31], the heat exchange between the two covers was neglected.

2.4. Back-pass solar air heater

In this design, the absorber plate is placed directly behind the transparent cover with a layer of static air separating it from the cover (Fig. 4). The air to be heated flows between the inner surface of the absorber and the layer of insulation [3]. Heat transfer in this design has been investigated by Choudhury and Garg [4], Ong [7], Hegazy [26], Garg et al. [32], Choudhury et al. [33], Al-Kamil and Al-Ghareeb [34], Jannot and Coulibaly [35], Hegazy [36].

Garg et al. [32] developed a simple mathematical model to investigate the performance of the system under different design and flow conditions. The energy balance equations for different components of the air heater were written as follows:

$$\text{For cover}: \quad h_{gs}(T_s - T_g) + h_{rpg}(T_p - T_g) = U_t(T_g - T_a) \quad (32)$$

$$\text{For absorber plate}: \quad (\alpha\tau)S = h_{cpf}(T_p - T_{fm}) + h_{rps}(T_p - T_a) + h_{rpb}(T_p - T_b) + h_{rpg}(T_p - T_g) \quad (33)$$

$$\text{For the flow air}: \quad h_{cpf}(T_p - T_{fm}) = h_{cbf}(T_{fm} - T_b) + mC_a(T_{fo} - T_a) \quad (34)$$

$$\text{Bottom plate}: \quad h_{rpb}(T_p - T_b) = h_{cbf}(T_b - T_{fm}) + U_b(T_b - T_a) \quad (35)$$

With a deal to compare theoretical parametric analysis of solar air heating collector with and without packing in flow passage above the rear plate, Choudhury et al. [4] investigated this design of solar air heater (Fig. 4). The steady state energy balance equations for different components are presented below:

$$\text{For cover}: \quad \alpha_g S + h_{rpg}(T_p - T_g) + h_{cpg}(T_p - T_g) = (h_w + h_{rs})(T_g - T_a) \quad (36)$$

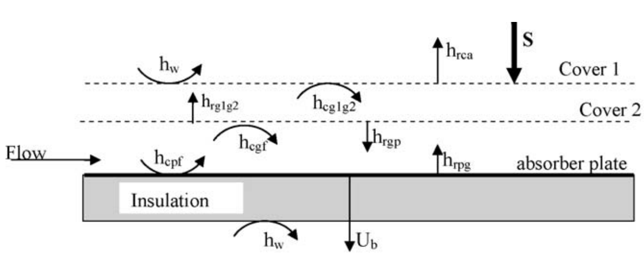


Fig. 3. A schematic view of a single cover solar air heater [7,9,16,31].

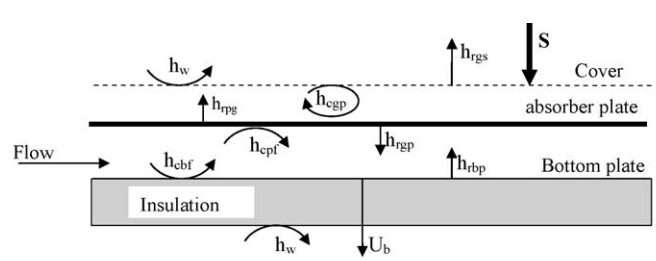


Fig. 4. A schematic view of a single cover solar air heater [7,16,26,31,32,36].

$$\text{For absorber plate}: \quad \alpha_p \tau_g S = h_{cpf}(T_p - T_f) + h_{cpg}(T_p - T_g) + h_{rpb}(T_p - T_b) + h_{rpg}(T_p - T_g) \tag{37}$$

$$\text{For the flow air}: \quad h_{cpf}(T_p - T_f) = h_{cbf}(T_f - T_b) + \frac{mC_f}{W}\frac{dT_f}{dx} \tag{38}$$

$$\text{Bottom plate}: \quad h_{cbf}(T_f - T_b) + h_{rpb}(T_p - T_b) = U_b(T_b - T_a) \tag{39}$$

The boundary conditions for the above sets of equations were $T_f(x=0) = T_{fi}$, $T_f(x=L) = T_{fo}$.

In the mathematical model written by Ong [7], there is no heat extracted from the system between the top cover and the stagnant air cavity. The air has been assumed to recirculate within the space under free convection in an inclined wall cavity. Hence the energy balance equations obtained for this design are the same as predicted by Choudhury and Garg [4] instead of Eq. (38) which has been replaced by

$$h_{cpf}(T_p - T_f) = h_{cbf}(T_f - T_b) + \frac{2mC_f}{WL}(T_f - T_{fi}) \tag{40}$$

In the investigation of Choudhury et al. [4] Eqs. (36), (37) and (39) should be considered without the terms of natural convection between cover-absorber plate and radiative exchange between cover-ambient. Eq. (37) is replaced by

$$\frac{mC_f}{W}\frac{dT_f}{dx} = h_{pf}(T_p - T_f) + h_{bf}(T_b - T_f) \tag{41}$$

This solar air heater model has also been investigated experimentally and theoretically by Al-Kamil and Al-Ghareeb [34]. They studied experimentally and theoretically the effect of solar radiation on the solar collector. The balance energy equations based on the subdivision concept were developed and for all the components of the solar air heater, were written as

$$\text{Flowing in the channel}: \quad h_{cpf}(T_{pi} - T_{fi})A_i = h_{cbf}(T_{fi} - T_{bi})A_i + mC_f(T_{f(i-1)} - T_{fi}) \tag{42}$$

$$\text{Absorber}: \quad (\alpha\tau)S + h_{cpf}(T_{pi} - T_f) + h_{nc}(T_{pi} - T_{gi}) + h_{rpb}(T_{pi} - T_{bi}) + h_{rpg}(T_{pi} - T_{gi}) = \rho_p V_p C_p \frac{T_{pi} - \bar{T}_{pi}}{A_i \Delta t} \tag{43}$$

$$\text{Glass cover}: \quad \alpha_g S F_{sh} F_d A_i + h_{rpg}(T_{pi} - T_{gi})A_i + h_{nc}(T_{pi} - T_{gi})A_i = (h_w + h_{rs})(T_{gi} - T_a)A_i \tag{44}$$

$$\text{For bottom plate}: \quad h_{cbf}(T_{fi} - T_{bi})A_i + h_{ba}(T_a - T_{bi})A_i + h_{rpb}(T_{pi} - T_{bi})A_i = 0 \tag{45}$$

where F_{sh} and F_d are shading and dust factors. The balance energy equations were solved by Gauss–Seidel iterations using a computer program written in BASIC. The heat transfer coefficients were determined by familiar methods available in the literature. The results have shown a closing agreement between predicted and measured data warrant the use of the subdivision method to predict some useful information about the radiation effect.

Another mathematical model for this design of solar air heater with a plastic film has been proposed by Jannot and Coulibaly [35]. They studied theoretically the evolution of the radiative fluxes inside the collector by a ray tracing method applied to each flux considering the different and successive reflections and absorptions occurring on absorber plate and on the transparent cover. The thermal analysis will result in the radiative balances of these two components. Assuming that the collector area is equal to 1 m^2, the net radiative flux received by these two components are stated as

For absorber:

$$\Phi_p = \frac{\alpha_{ps}\tau_{gs}}{1-\rho_{gs}(1-\alpha_{ps})}S + \frac{\alpha_{gi}\alpha_{pi}}{1-\rho_{gi}(1-\alpha_{pi})}\sigma T_g^4 + \frac{\tau_{gi}\alpha_{pi}}{1-\rho_{gi}(1-\alpha_{pi})}\Phi_{sky} + \frac{\rho_{gi}\alpha_{ci}}{1-\rho_{gi}(1-\alpha_{pi})}\sigma T_p^4 - \sigma\frac{T_p^4 - T_b^4}{(1/\alpha_{pi}) - (1/\alpha_{bi}) - 1} - \sigma\alpha_{pi}T_p^4 \tag{46}$$

For transparent cover:

$$\Phi_g = S\alpha_{gs} + \frac{\alpha_{gs}\tau_{gs}(1-\alpha_{ps})}{1-\rho_{cs}(1-\alpha_{ps})}S + \frac{\alpha_{gi}\alpha_{gi}(1-\alpha_{pi})}{1-\rho_{gi}(1-\alpha_{pi})}\sigma T_g^4 + \left[\frac{\tau_{gi}\alpha_{gi}(1-\alpha_{pi})}{1-\rho_{gi}(1-\alpha_{pi})} + \alpha_{gi}\right]\Phi_{sky} + \frac{\alpha_{pi}\alpha_{gi}}{1-\rho_{gi}(1-\alpha_{pi})}\sigma T_p^4 - 2\sigma\alpha_{gi}T_g^4 \tag{47}$$

in the case of a transparent cover opaque to IR, $\tau_{gi} = 0$ and $\rho_{gi} = 1 - \alpha_{gi}$. Eqs. (46) and (47) become:

$$\Phi_p = \frac{\alpha_{ps}\tau_{gs}}{1-\rho_{gs}(1-\alpha_{ps})}S + \sigma\frac{T_p^4 - T_g^4}{1/\alpha_{pi} - 1/\alpha_{gi} - 1} - \sigma\frac{T_p^4 - T_b^4}{1/\alpha_{pi} - 1/\alpha_{bi} - 1} \tag{48}$$

and

$$\Phi_g = S\alpha_{gs} + \frac{\alpha_{gs}\tau_{gs}(1-\alpha_{ps})}{1-\rho_{cs}(1-\alpha_{ps})}S + \sigma\frac{T_p^4 - T_g^4}{1/\alpha_{pi} - 1/\alpha_{gi} - 1} + \sigma\alpha_{gs}(\varepsilon_a T_a^4 - T_g^4) \tag{49}$$

The results showed that the modifications induced by taking into account the partial transparency of the cover towards IR radiation may be important.

Another investigation has been published by Hegazy [36]. In this model, Eq. (16) is reconsidered for the cover balance equation, with $T_{fm}(=(T_{fi} + T_{fo})/2))$ replaced by T_p and the hg becomes h_{cpg}. Energy balance on the bottom plate was written as Eq. (35). U_b is recalled in Table 1. For the others components of the design, energy balance equations have been written as

$$\text{For absorber plate}: \quad \alpha_p \tau_g S = h_{cpf}(T_p - T_{fm}) + (h_{cpg} + h_{rpg})(T_p - T_g) + h_{rpb}(T_p - T_b) \tag{50}$$

$$\text{For the air flow}: \quad h_{cpf}(T_p - T_{fm}) = h_{cbf}(T_{fm} - T_b) + 2GC_p\frac{(T_{fm} - T_{fi})}{(L/dx)} \tag{51}$$

In order to demonstrate the engineering accuracy of the proposed criterion, the author has determined the absorber mean temperature at the exit. To accommodate this necessity, energy balances (35), (50) and (51) have been applied progressively to each element and solved iteratively. It was concluded that the channel ratio (D/L) plays a decisive role in determining the rate of useful heat gain.

To determine the flow channel optimum geometry and study the effect of the variation in the absorber width on both the thermal and hydraulic performance of this design, two new mathematical models have been published by Hegazy [17,26]. In these new models, all energy balance equations proposed by this author in 1999 are reconsidered instead of the equation of the air

Table 1
A review of heat transfer coefficient used in different models.

References	Solar air heaters systems	Heat transfer coefficients
Choudhury et al. [4]	A bare plate solar air heater	The radiative and natural convective coefficients were summarized in Duffie and Beckmann [5] h_{pf} and h_{bf} [6]: $h_f = \mathrm{Nu}_\infty(1 + MD/L)k/D$ with $\mathrm{Nu}_\infty = 0.0182Re^{0.8}Pr^{0.4}$ and $M = 14.3\log_{10}(N) - 7.9$. $N = L/D$ if $0 < L/D \le 60$ and $N = 60$ if $L/D > 60$.
Njomo [8] & Njomo and Daguenet [9]		$h_{c\,pa} = 0.86\,Re^{1/2}Pr^{1/3}(k_p/L_p)$, with $L_p = 4WL/2W + 2L$ for rectangular plates and with $2 \times 10^4 < \mathrm{Re} < 6 \times 10^4$ [10]. Duffie and Beckmann [5] suggested that the above equation is valid for $\mathrm{Re} > 10^6$. h_{cpf} and h_{cbf} (see [11]): for the laminar flow ($\mathrm{Re} < 2100$): $\mathrm{Nu} = h_c\mathrm{Dh}/K_f = 4.9+$ $(0.0606(RePr\mathrm{Dh}/L)^{1.2}/1 + 0.0909(RePr\mathrm{Dh}/L)^{0.7}Pr^{0.17})$ for turbulent flow ($\mathrm{Re} > 2100$) by [5]: $\mathrm{Nu} = h_c\mathrm{Dh}/K_f = 0.0158Re^{0.8}$ with $\mathrm{Dh} = 4WD/2W + 2D$ $h_{r\,pa} = \sigma\varepsilon_p(T_p^4 - T_{sky}^4)/(T_p - T_a)$, where $T_{sky} = T_a[0.787 + 0.0028(T_d - 273)]^{0.25}$ [12] and T_d is the dew point temperature of the ambient air; it is related to its water vapor pressure e_{mb} (in millibars) and has been calculated from: $e_{mb} = 1013.25/760\exp(20.519 - 5179.25/T_d)$, $h_{rb\,p} = \sigma(T_p + T_b)(T_p^2 + T_b^2)/(2/\varepsilon_p) - 1$
Garg et al. [13]	Single one cover solar air heater	The important dimensions and the heat transfer parameters used were given in McAdams [19], Kreith and Kreider [20]
Ong [7]		The radiation coefficient between parallel plates set i–j is given as: $h_{rij} = \sigma(T_i + T_j)(T_i^2 + T_j^2)/(1/\varepsilon_i) + (1/\varepsilon_j) - 1$ The forced convection heat transfer coefficient between parallel plates is given: for laminar flow ($\mathrm{Re} < 2300$) [21] $h\mathrm{Dh}/k = 5.4 + 0.00190(\mathrm{RePrDh}/L)^{1.71}/1 + 0.00563(\mathrm{RePrDh}/L)^{1.71}$, for transition flow region ($2300 < \mathrm{Re} < 6000$) [22]: $(hd_h/k) = 0.116(Re^{2/3} - 125)Pr^{1/3}[1 + (D_h/L)^{2/3}](\mu/\mu_w)^{0.14}$ and for turbulent flow ($\mathrm{Re} > 6000$) [23] $(h\mathrm{Dh}/k) = 0.018\,Re^{0.08}Pr^{0.4}$, the heat transfer coefficient at the entrance region is computed with the same relation as h_{pf} (see [4]), $h_{rs} = \sigma\varepsilon_g(T_g^4 - T_s^4)/(T_g - T_a)$
Naphon and Kongtragool [17]		The convective heat transfer coefficient is computed using [24]: $\mathrm{Nu} = (h\mathrm{Dh}/k) = 0.333\,Re^{0.8}\,Pr^{1.3}$ with $\mathrm{Dh} = 4WB/2W + 2B$
Hegazy [16]		h_{cpf} and h_{cgf} are computed with [6]: $h = k/\mathrm{Dh}\{0.0158Re_{\mathrm{Dh}}^{0.8} + (0.00181Re_{\mathrm{Dh}} + 2.92)\exp(-0.0379x/\mathrm{Dh})\}$ where $Re_{\mathrm{Dh}} = 2M/(1 + D/W)$ Dh is hydraulic diameter and M is a mass flow parameter. $U_b = [1 + 2(\delta_{in} + D + \delta_g/W)][\delta_{in}/k_{in} + 1/h_w]^{-1}$, δ_{in} and δ_g are the thickness of insulation and glass cover. The radiative heat transfer coefficient (see Ong [7])
Aboul-Enein et al. [27]		h_{cpf} and h_{cfh} were computed using [28]: $\mathrm{Nu} = h_{cpg}\mathrm{Dh}/k = 1 + 1.44[1 - 1708/R_a\cos(\beta)]^+ + [1 - 1708(\mathrm{Sin}(1.8\beta))^{1.6}/R_a\,\mathrm{Cos}(\beta)] + [(R_a\cos(\beta)/5830)^{1/3} - 1]^+$ where $[\ ]^+$ means that only positive values are taken into account. β is a collector tilt angle. h_{rpg} (see Ong [7]) and $h_{rgs} = \sigma\varepsilon_g(T_g^2 + T_{skys}^2)(T_g - T_{sky})$
Njomo [14] and Njomo and Daguenet [9]		h_{cgp}, h_{rpa}, h_{cpf} (see Choudhury et al. [4]) $h_{rij} = \sigma\varepsilon_p((1 - \rho_g)T_p^4 - \beta_g T_g^4)/(1 - \rho_p\rho_g)(T_p - T_g)$ and $h_{r\,pa} = \sigma\varepsilon_p\tau_{ir}(T_p^4 - T_{sky}^4)/(T_p - T_a)$
Naphon and Kongtragool [17]	Single two covers solar air heater	$h_{rg1a} = \sigma(T_{g1} + T_a)(T_{g1}^2 + T_a^2)/((1/\varepsilon_{g1}) - 1)$, h_{rpg} (see [7]) with $i = p$ and $j = g$
Garg et al. [32]	Back-pass solar air heater	The radiative heat transfer coefficients (see Ong [7]) The convective heat transfer coefficient from the upper plate to the flowing air and the pressure drop [37]: $\mathrm{Nu} = 2bh/k = \mathrm{Nu}_0 + \beta(b/L)$, $\Delta P = [f_0 + \gamma(b/L)(m^2/\rho)(L/b)^3]$, for $\mathrm{Re} < 2550$ (laminar flow) $\mathrm{Nu}_o = 5.385$; $\beta = 0.0148\mathrm{Re}$; $f_0 = 24/\mathrm{Re}$; $\gamma = 0.9$; for $2550 < \mathrm{Re} < 10^4$ (transitional flow) $\mathrm{Nu}_o = 4.4 \times 10^{-4}Re^{1.2}$; $\beta = 9.37\,Re^{0.471}$; $f_0 = 0.0094$, $\gamma = 2.92\,Re^{-0.15}$; for $10^4 < \mathrm{Re} < 10^5$ (early turbulent flow) $\mathrm{Nu}_o = 0.03Re^{0.74}$; $\beta = 0.788\,Re^{0.471}$; $f_0 = 0.059\,Re^{-0.2}$; $\gamma = 0.73$.
Choudhury and Garg [87]		h_{cpf} and h_{cbf} (see [17]) other heat transfer coefficients (see [5])
Hegazy [36]		$U_b = [1 + (2/W)(\delta_{in} + D + S - \delta_g)][\delta_{in}/k_{in} + 1/h_w]^{-1}$, h_{cpg} (see [27]) h_{cpf} and h_{cbf} is correlated by (see Biehl [38]): $h = k/\mathrm{Dh}\{0.015Re_{\mathrm{Dh}}^{0.8} + (0.00181Re_{\mathrm{Dh}} + 2.92)\exp(-0.03795x/\mathrm{Dh})\}$
Jha et al. [43]	Parallel-pass solar air heater: Type 1	The forced convection heat transfer coefficient between air and plate or between air and cover is obtained by using the equation [24]: $h = 0.0293\,Re^{0.8}k_f/D$. The natural convection heat transfer coefficient (see Wong [41])
Ong [7]		The radiative heat transfer coefficients and the forced convection heat transfer between parallel plates for laminar flow, transition flow region and turbulent flow (see Ong [7]). For $9500 < \mathrm{Re} < 22000$, situations involving a large property variation [42] $\mathrm{Nu} = (h_{\mathrm{Dh}}/k) = 0.027\,Re^{0.8}Pr^{1/3}(\mu/\mu_w)^{0.14}$
Hegazy [16,26]		h_{cpf1}, h_{cgf1}, h_{cbf2}, h_{cpf2} were calculated using the following equation: $h = (k/D_{hj})\{0.015Re_j^{0.8} + (0.00181Re_j + 2.92)\exp(-0.03795x/D_{hj})\}$, $U_b = [1 + 2(\delta_{in} + D_1 + D_2 + \delta_g/W)][\delta_{in}/k_{in} + 1/h_w]^{-1}$ W was replaced by the average width $\bar{W}(x)$ in the second model [26]
Forson et al. [3]		Radiative heat transfer coefficients (see [7–9]), free convective heat transfer coefficient (see [16]), $U_{ej} = (UA)_{\mathrm{edge}}/A_c = \{(k/x)S_j\}/W$
Yel et al. [45]	Parallel-pass solar air heater: Type 2	$\left\{U_{g1a}^{-1} = U_T^{-1} - (h_{rpg1}^{-1} + h_{cpf1}^{-1})^{-1}\right\}$ or $U_{g1a}^{-1} = (h_w + h_{rg2a})^{-1} - (h_{cg1g2}^{-1} + h_{rg1g2}^{-1})^{-1}$ where $h_{cg1g2} = 1.25(T_{fm1} - T_{fm2})^{0.25}$, $h_{rpg1} \approx 4\sigma T_{fm1}^3/[\varepsilon_p^{-1} + \varepsilon_{g1}^{-1} - 1]$, $h_{rpb} \approx 4\sigma T_{fm2}^3/[\varepsilon_p^{-1} + \varepsilon_b^{-1} - 1]$ h_{rg1g2}, h_w (see Ong [7] and (A1)), $h_{rg2a} = \sigma\varepsilon_g(T_{g2m} + T_a)(T_{g2m}^2 + T_a^2)$ $U_B^{-1} = U_b^{-1} + h_{cbf2}^{-1} + l_B k_B^{-1}$ and $U_b \approx k_s l_c^{-1}$

		The forced convection heat-transfer coefficient between two flats plates: for laminar flow in a short conduct [21]: $Nu_j = D_h h_j/k = 4.4 + 0.00398(0.7 Re_j Pr Dh/L)^{1.66}/1 + 0.0114(Re_j Pr Dh/L)^{1.12}$ (j = 1, 2), while for turbulent flow [19,46] data: $Nu_j = (D_h h_j/k) = 0.018 Re_j^{0.08}[1 + (D_e/L)^{0.7}]$
Matrawy [49]	Solar air heater with slats	$U_t = [1/(h_{nc} + h_{r1c}) + 1/(h_w + h_{rca})]^{-1}$
Ammari [51]		$h_{rca} = \sigma\varepsilon_c(T_c + T_s)(T_s^2 + T_c^2)(T_c - T_s/T_c - T_a)$, h_{rpg} and h_{rga} (see [7]), Natural convection (see [27]), inner surface convective coefficients (see [7–9])
Wijeysundera et al. [57]	Two-pass solar air heaters	$U_{21} = [(1/h_{cg1f}) + (1/h_{cg2f})]^{-1}$, $h_{rij} = \sigma h_{ij}\left(T_i^2 + T_j^2\right)(T_i + T_j)$, $h_{cij} = C_{ij}(T_i + T_j)$.
Verma et al. [59]		The convective heat transfer coefficient between enclosed spaced (see [27]) The forced convective heat transfer coefficient (see [8,9])
Naphon and Kongtragool [17]		The heat transfer coefficient (Niles et al. [24]): $N_u = hD/k = 0.0333\ Re^{0.8}Pr^{1/3}$.
Zhai et al. [18]		h_{g1a} = convection heat transfer from glazing due to wind (see Eq. (A1)) + radiation heat transfer coefficient from glass cover to sky referred to the ambient air temperature(see [8,9]). The global heat transfer coefficient from insulation plate to the attic: $U_b = [1/h_{cbattic} + \Delta b/k_b]$
Yamali and Solmus [63]		h_{rg2sky} (see [8,9]), h_{rg1g2} (see [7]), h_{cg1g2} (see [28]), h_{cg1f1} (see [8,9]) for laminar flow and (see [64]): $Nu_{g1f1} = (f_{f1}/8)(Re_{f1} - 1000)Pr/1 + 12.7(f_{f1}/8)^{0.5}(Pr^{0.67} - 1)$ with $f_{f1} = \sqrt{0.79 \ln Re_{f1} - 1.64}$.
Ho et al. [66]	Double-pass flat-plate solar air heater with recycle	$h_1 = h_1'$, $h_2 = h_2'$. The forced convection heat transfer between two plates (see Kays [46]), for a short conduit h_1 and h_2 (see [19]): $N_{u,f} = h_j D_e/k = 0.0158 R_{e,f}^{0.8}\left[1 + (D_e/L)^{0.7}\right](j = 1, 2)$, for the laminar flow (see Heaton et al. [21]), h_T (see [67,68] and Eq. (A4)). $1/h_B = 1/h_{B1s} + 1/h_2' + l_B/k_B \quad 1/U_{gls} = 1/h_{rg2s} + h_w + 1/h_{cg1g2} + h_{rg1g2}$ or $1/U_{gls} = 1/U_T + 1/h_{rpg1} + h_1$ where $h_{cg1cg2} = 1.25(T_{g1m} - T_{g2m})^{0.25}$ (see [67]), $h_{rpg1} = 4\sigma T_{bm}^3/[(1/\varepsilon_p) + (1/\varepsilon_p) - 1]$ $h_{rpR} = 4\sigma T_{am}^3/[(1/\varepsilon_p) + (1/\varepsilon_R) - 1]$, those between two glass covers (see Ong [7]) and from cover 2 to ambient: $h_{rg2s} = \sigma\varepsilon_g(T_{g2}^2 + T_{sky}^2)(T_{g2} + T_{sky})$.
Naphon [71]	Double-pass flat plate solar air heater with longitudinal fins	The convective heat transfer coefficient between channel (see [7,17]).
Chandra et al. [72]	Triple pass solar air heaters	The radiative heat transfer coefficient between two surfaces i and j (see Ong [7]) and the convective heat transfer coefficient (See [73]): $Nu = h_f D/k = 0.036 \quad Pr^{0.8}Pr^{0.8}$
Ho et al. [76]	Multi-pass flat-plate solar air heaters with external recycle	$h_1 = h_1'$, $h_2 = h_2'$, $h_3 = h_3'$, $and\, h_4 = h_4'$, . Other coefficients (see Ho et al. [66])
Tchinda [78]	Solar air heater with a compound parabolic concentrator	$h_{r1} = \sigma(T_C^2 + T_v^2)(T_C + T_v)/1/\varepsilon_v + A_V/A_C(1/\varepsilon_C - 1)A_C/A_p$, $h_{r2} = \sigma\varepsilon_C(T_C^2 + T_S^2)(T_C + T_S)A_C/A_p$, $h_{v/C} = (3.25 + 0.0085T_v - T_C/2D_v)A_v/A_p$ (see [79]) with $D_v = 2l_v(e_f + e_{pv})/l_v + e_f + e_{pv}$ U_f (see [5,11,81])
Karim and Hawlader [83]	v-Groove solar air collector	The convective heat transfer coefficient within the airflow duct (see [61]): $Nu = Nu_0 + n\beta b/L$, For laminar flow ($Re < 2800$): $Nu_0 = 2.821$, $\beta = 0.126$ Re; For transition flow ($2800 \le Re < 10^5$): $Nu_0 = 1.9 \times 10^{-6}Re^{1.79}$, $\quad \beta = 225$; For turbulent flow ($10^4 < Re < 10^5$): $Nu_0 = 0.030210^{-6}Re^{0.74}$, $\quad \beta = 0.242\,Re^{0.74}$. the top loss coefficient U_t, (see Klein [67])
Bashria et al. [84–86]		The radiative coefficient from absorber to the cover [52,87]: $h_r = \sigma(T_p^2 + T_g^2)(T_P + T_g)/1/\varepsilon_{p'} + 1/\varepsilon_g - 1 \quad$ with $\varepsilon_{p'} = 2\varepsilon_p/1 - \varepsilon_p$; The convective heat transfer (see [7]), with $Dh = 2H_v\sin(\theta/2)/1 + \sin(\theta/2)$
Choudhury and Garg [88]	Single pass solar air heater with packed, type 1	h_{cpf}, h_{cbf} and h_{cp1f}, (see [89]): $hcpf = h_{cbf} = 0.2Re_{p1}^{0.8}Pr^{1/3}k_f D_p^{-1}$, $h_{cp1f} = [1/h_{p1f} + D_P/Wk_{p1}]^{-1}$, with $h_{p1f} = 0.255Re_{p1}^{0.8}P_r^{1/3}k_f D_p^{-1} \in^{-1}$. For the other heat transfer coefficients (see [5]).
Choudhury and Garg [88]	Single pass solar air heater	For all the heat transfer coefficients (see [88,90,91,95])
El-Sebaii et al. [99]	with packed, type 2	For the various heat transfer coefficients (see [97])
Ramadan et al. [96]	Double-pass solar air heater with packed	$h_{cg1f1}Nu_{p1}k_{f1}/D_e = 0.2Re_{p1}^{0.8}Pr^{1/3}k_{f1}/D_e$ (see [98]), with $Re_{p1} = m_f D_e/\mu A_{p1}$, $D_e = (2/3)[\varepsilon D_{p1}/(1 - \varepsilon)]$, ε is porosity of the packed bed ($\varepsilon < 1$): $\varepsilon = (V_{chan} - V_{p1})/V_{chan}$, V_{chan} and V_{p1} are the total volume of the channel and the volume of the packed bed material. $D_{p1} = 6V_S^{1/3}/n\pi$ (see [97]) V_s = total volume of n particles selected randomly. $A_{p1} = 6(1 - \varepsilon)/D_{p1}$ (see [97]). $h_{pf1} = h_{cg1f1}$ (see [43]), $h_{cp1f1} = [1/h_{p1f} + D_e/D_{p1}S_{p1}]^{-1}$ (see [90]) with $N_{p1f} = h_{p1f}D_e/k_{f1} = (0.255/\varepsilon)Re_{p1}^{2/3}Pr^{1/3}$, S_{p1} is a constant and depends on the packed bed shape.

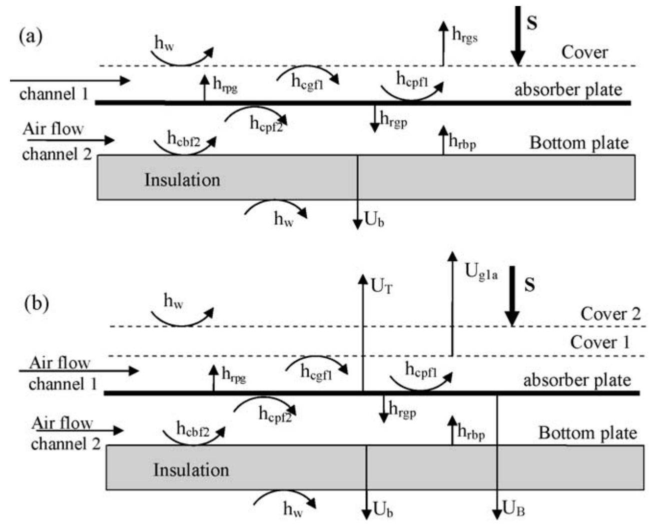


Fig. 5. (a) A schematic view of a single cover solar air heater [7,16,26,32,36]. (b) A schematic view of a single cover solar air heater [45].

flow which has been replaced respectively by Eq. (17) and:

$$h_p(T_p - T_{fm}) = h_{cbf}(T_{fm} - T_b) + 2GC_p\frac{(T_{fm} - T_{fi})}{(A_P/A(x))} \tag{52}$$

with Re = $4m/\mu P(x)$ and Dh = $4W(x)D/P(x)$.

2.5. Parallel-pass solar air heater

2.5.1. Type 1

The solar air heater configuration under consideration is shown in Fig. 5a. It consists of one cover, double channel design with double air flows between cover and absorber plate and between absorber and bottom plates and with insulation provided. Many papers have investigated this design [7,16,17,26,39,40,43].

Jha et al. [43] obtained the energy balance equations in partial differential forms, which govern the behavior of the system, by considering energy conversation at each component of the system separately. For the solar heater shown in Fig. 5a, the following equations were obtained:

$$\text{At the cover}: \quad M_gC_g\frac{\partial T_g}{\partial t} = \alpha_g S + h_{rpg}(T_p - T_g) + h_{cf1g}(T_{f1} - T_g) - h_{cgw}(T_g - T_w) - h_{rga}(T_g - T_a) \tag{53}$$

For air flowing between cover and plate absorber :

$$M_{f1}C_f\frac{\partial T_{f1}}{\partial t} = \frac{-G_1C_f}{W}\frac{\partial T_{f1}}{\partial x} + h_{cpf1}(T_p - T_{f1}) - h_{cf1g}(T_{f1} - T_g) \tag{54}$$

$$\text{For Plate 1}: \quad M_1C_p\frac{\partial T_p}{\partial t} = \alpha_p\tau_g S - k_p\delta_p\frac{\partial^2 T_p}{\partial x^2} - h_{rpg}(T_p - T_g) - h_{cpf2}(T_p - T_{f2}) - h_{rpb}(T_p - T_b) - h_{cpf1}(T_p - T_{f1}) \tag{55}$$

For air flowing between absorber plate and bottom plate :

$$M_{f2}C_f\frac{\partial T_{f2}}{\partial t} = \frac{-G_2C_f}{W}\frac{\partial T_{f2}}{\partial x} + h_{cpf2}(T_p - T_{f2}) - h_{cbf2}(T_b - T_{f2}) \tag{56}$$

$$\text{For bottom plate}: \quad M_bC_b\frac{\partial T_b}{\partial t} = -k_b\delta_b\frac{\partial^2 T_b}{\partial x^2} + h_{rpb}(T_p - T_b) - h_{cbf2}(T_b - T_{f2}) - h_b(T_b - T_r) \tag{57}$$

The boundary and initial conditions are given by the following equations:

$$\left.\frac{\partial T_p}{\partial x}\right|_{x=0} = 0, \qquad \left.\frac{\partial T_p}{\partial x}\right|_{x=L} = 0, \qquad \left.\frac{\partial T_b}{\partial x}\right|_{x=L} = 0 \tag{58a}$$

$$T_{f1}(x=0) = T_{fi},\ T_{f2}(x=0) = T_{fi} \tag{58b}$$

Ong [7] obtained from the thermal network the following heat balance equations:

$$\text{For cover}: \quad \alpha_g S + h_{rpg}(T_p - T_g) + h_{cgf1}(T_{f1} - T_g) = (h_w + h_{rs})(T_g - T_a) \tag{59}$$

For air flow between cover and the absorber plate :

$$h_{cpf1}(T_p - T_{f1}) = h_{cgf1}(T_{f1} - T_g) + 2m_1C_f\frac{T_{f1} - T_{if1}}{WL} \tag{60}$$

$$\text{For absorber plate}: \quad \alpha_p\tau_g S = h_{cpf2}(T_p - T_{f2}) + h_{rpg}(T_p - T_g) + h_{rpb}(T_p - T_b) + h_{cpf1}(T_p - T_{f1}) \tag{61}$$

For air flow between absorber plate and the bottom plate :

$$h_{cpf2}(T_p - T_{f2}) = h_{cbf2}(T_{f2} - T_b) + 2m_2C_f\frac{T_{f2} - T_{if2}}{WL} \tag{62}$$

With the aim to determine the channel optimum geometry of the flat plate and to study the effect of the variation in the absorber width on both the thermal and hydraulic performances of this solar air heater (Fig. 5a), Hegazy [16,26] has written two mathematical models. In the two models, the energy balance equations on the glass cover, the absorber plate and the bottom plate are given as

$$\alpha_g S + h_g(T_{fm1} - T_g) + h_{rpg}(T_p - T_g) = (h_w + h_{rgs})(T_g - T_a) \tag{63}$$

$$\alpha_p\tau_g S = h_{cpf1}(T_p - T_{fm1}) + h_{rpg}(T_p - T_g) + h_{cpf2}(T_p - T_{fm2}) + h_{rpg}(T_p - T_b) \tag{64}$$

$$h_{cbf2}(T_{fm2} - T_b) + h_{rpb}(T_p - T_b) = U_b(T_b - T_a) \tag{65}$$

The energy balance equation of the air flow in the upper and the lower channel are

$$\text{For the first model}: \quad h_{pf1}(T_p - T_{fm1}) = h_g(T_{fm1} - T_g) + 2G_1C_p\frac{T_{fm1} - T_{if1}}{(L/dx)} \tag{66}$$

$$h_{pf2}(T_p - T_{fm2}) = h_{bf2}(T_{fm2} - T_b) + 2G_2C_p\frac{T_{fm2} - T_{if2}}{(L/dx)} \tag{67}$$

$$\text{For the second model}: \quad h_{pf1}(T_p - T_{fm1}) = h_g(T_{fm1} - T_g) + 2G_1C_p\frac{T_{fm1} - T_{if1}}{(A_p/A(x))} \tag{68}$$

$$h_{pf2}(T_p - T_{fm2}) = h_{bf2}(T_{fm2} - T_b) + 2G_2C_p\frac{T_{fm2} - T_{if2}}{(A_p/A(x))} \tag{69}$$

with Re = $4m/\mu P$ and Dh = $4W/P$ for model 1 [16], Re = $4m/\mu P_j(x)$ and $D_h = 4\bar{W}(x)/P_j(x)$ for the second model [26].

To study the performance of this solar design (Fig. 5a), Naphon and Kongtragool [17] proposed another mathematical model. This model is characterized by the following equations:

$$\text{For the cover}: \quad \alpha_{g1}S = h_w(T_{g1} - T_a) + h_{cf1g1}(T_{g1} - T_{f1}) + h_{rg1p}(T_{g1} - T_p) + h_{rag1}(T_{g1} - T_a) \tag{70}$$

$$\text{For the air flow between upper cover and absorber}: \quad mC_f\frac{dT_{f1}}{dx} = h_{cg1f1}(T_{g1} - T_{f1}) + h_{cpf1}(T_p - T_{f1}) \tag{71}$$

For the absorber plate : $\alpha_p \tau_{g1} S$
$$= h_{cf1p}(T_p - T_{f1}) + h_{cf2p}(T_p - T_{f2}) + h_{rg1p}(T_p - T_{g1}) + h_{rpb}(T_p - T_b) \quad (72)$$

For the air flow in lower channel : $mC_f \frac{dT_{f2}}{dx}$
$$= h_{cf2p}(T_p - T_{f2}) + h_{cf2b}(T_b - T_{f2}) \quad (73)$$

For the bottom plate : $h_{cf2b}(T_b - T_{f2}) + h_{rpb}(T_b - T_p)$
$$+ U_b(T_b - T_a) = 0 \quad (74)$$

Forson et al. [43] have investigated theoretically and experimentally heat transfer in the design shown in Fig. 5a. Making a general assumption, Forson et al. [43] formulated the equations governing the performance of the system by coupling the energy equations of the components of the solar air heater with those for the useful heat extracted in the two channels. The energy balance equations for various components of the system are given below:

For the cover : $\bar{S}_g = h_w(T_{g1} - T_a) + h_{rcs}(T_g - T_s)$
$$+ h_{rpg}(T_g - T_p) + h_{cgf1}(T_g - T_{f1}) \quad (75)$$

For the air flow between upper cover and absorber:

$$m_1 C_f \frac{dT_{f1}}{dx} = Wh_{cpf1}(T_p - T_{f1}) + Wh_{cgf1}(T_g - T_{f1}) + U_{egs1}(T_a - T_{f1}) \quad (76)$$

For the absorber plate:

$$\bar{S}_p = h_{cpf2}(T_p - T_{f2}) + h_{cpf1}(T_p - T_{f1}) + h_{rpb}(T_p - T_b) + h_{rpg}(T_p - T_g) \quad (77)$$

For the air flow in lower channel:

$$m_2 C_f \frac{dT_{f2}}{dx} = Wh_{cf2b}(T_b - T_{f2}) + Wh_{cpf2}(T_b - T_{f2}) + U_{es2}(T_a - T_{f2}) \quad (78)$$

For the bottom plate:

$$h_{cf2b}(T_b - T_{f2}) + h_{rpb}(T_b - T_p) + U_b(T_b - T_a) = 0 \quad (79)$$

The pressure drop is given by Achenbach and Cole [44]:

$$D_t = 233.9 h \rho_a \left(\frac{T_{fm} - T_a}{T_{fm}} \right) \quad (80a)$$

with

$$T_{fm} = \frac{5}{9}[T_a - 0.65(T_a - T_{fo})] \quad (80b)$$

and

$$h = L\sin(\beta) \quad (80c)$$

The mass flow rate of air in each of the two channels is given by

$$m_j = W\rho_j s_j C_{vj} \sqrt{\frac{2D_{hj}}{fL\rho_j} \left\{ 233.9 h \rho_a \left(\frac{T_{fo} - T_a}{T_{fo} + \frac{7T_a}{13}} \right) \right\}} \quad (81)$$

Dh_j is the hydraulic mean depth of the duct and C_{vj} the coefficient of the velocity. The edge heat losses are estimated by assuming one dimensional sideways heat flow around the perimeter of the collector system. In Eqs. (75) and (77) $\bar{S}_g$ and $\bar{S}_p$ are given by the following:

$$\bar{S}_g = \alpha_g \overline{RK}_T \frac{\bar{H}_o}{3600 N_{ds}} \quad (82)$$

$$\bar{S}_p = \zeta \bar{R}' \left(a'' + b'' \frac{n}{\bar{N}} \right) \frac{\bar{H}_o}{3600 N_{ds}} \quad (83)$$

with

$$\bar{H}_o = \frac{24 \times 3600}{\pi} G_{sc} \left(1 + 0.033 Cos\left(\frac{360\bar{n}}{365} \right) \right) \left[Cos(\Phi) Sin(\delta) \sin\omega_s + \frac{\pi\omega_s}{180} + Sin(\Phi) Sin(\delta) \right] \quad (84)$$

A FORTRAN computer program was written and used to solve the above set of equations. In the solution procedure it was assumed that the air heater is subject to a constant insulation and hence, the plate temperature is constant. It was shown that significant improvement in solar air heater performance can be obtained with an appropriate choice of the collector parameters and the top to bottom channel depth ratio of the two ducts. The mass flow rate was shown to be the dominant factor in determining the overall efficiency of the heater.

2.5.2. Type 2

The energy flow diagram of such a device is presented in Fig. 5b. At seen in Fig. 5b, two air streams of different flow rates but with total flow rate fixed, are flowing steadily and simultaneously through two separate channels (above and below the absorbing plate). With the presence of the second cover, this device is different to the one of Fig. 5a. Yel et al. [45] investigated heat transfer in this design. In the mathematical model proposed by these authors, the following assumptions have been considered: the temperatures of absorbing plate, bottom plate and bulk fluids were functions of the flow direction only, and both the covers and fluid do not absorb radiant energy. The energy balances within the differential length *dx*, were given as

For inner cover : $h_{rpc1}(T_p - T_{g1}) + h_{cg1f1}(T_{f1} - T_{g1})$
$$= U_{g1a}(T_{g1} - T_a) \quad (85)$$

Absorbing plate : $\alpha_p \tau_g^2 S = U_T(T_p - T_a) + U_B(T_p - T_a)$
$$+ h_{CPF1}(T_p - T_{f1}) + h_{CPF2}(T_p - T_{f2}) \quad (86)$$

For the bottom plate : $h_{cbf2}(T_{f2} - T_b) + h_{rpb}(T_p - T_b)$
$$= U_b(T_b - T_a) \quad (87)$$

For fluid 1 : $rmC_f \frac{dT_{f1}}{dx} = Wh_{cpf1}(T_p - T_{f1})$
$$+ Wh_{cgf1}(T_g - T_{f1}) + h_{cf1g1}(T_{f1} - T_{g1}) \quad (88)$$

For fluid 2 : $(1 - r)mC_f \frac{dT_{f1}}{dx}$
$$= Wh_{CPF2}(T_p - T_{f2}) + Wh_{cbf2}(T_b - T_{f2}) \quad (89)$$

2.6. Solar air heater with slats

Yeh et al. [47] have presented a mathematical model for double flow solar air heaters with fins attached. Fig. 6a shows the design of a solar air heater with fins attached in which the absorbing plate divides the air conduit into two parts, channel 1 and 2. The energy flow diagram of such a device is also presented. As seen, two air flow of different mass flow rate but with total rate fixed, flow steadily and simultaneously through two such separated channels of the same size for heating. The method for theoretical prediction of collector efficiencies as well as the experimental procedure was

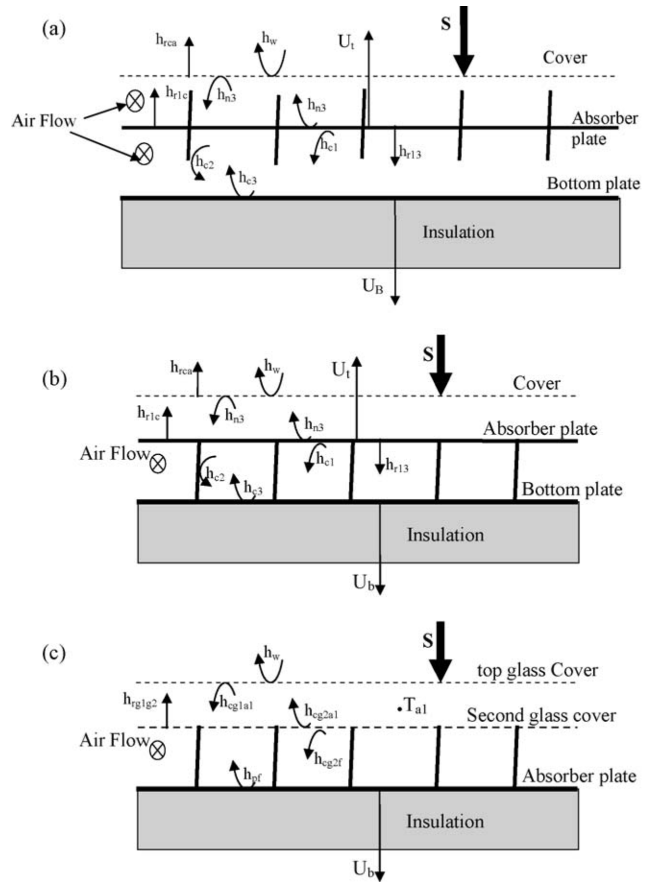


Fig. 6. (a) Schematic view studied by Yeh et al. [47]. (b) Schematic view studied by Ammari [51]. (c) Schematic view studied by Kabeel and Mecarik [50].

similar to that presented by the same authors [45], except that the allowance was for the fins to be attached to the upper and lower surfaces of the absorbing plate. It was shown that providing fins attached on the collector, will improve the collector efficiency and that the application of the concept of double flow in the design of a solar air heater with fins attached was technically and economically feasible.

Al-Nimr and Damseh [48], Matrawy [49], Kabeel and Mecarik [50] and Ammari [51] have investigated a solar air heater system that has metal slats connecting the absorber plate to the bottom plate as a development to enhance the thermal performance of the solar heater (Fig. 6b).

With the aim to study the dynamic performance of this design of solar air heater, Al-Nimr and Damseh [48] developed a mathematical model on the base of the following assumptions: (i) there are two separate phases, fluid and solid, which are not in thermal equilibrium. This was the case for low thermal conductivity fluid and low volumetric heat transfer coefficient between the fluid and solid domains; (ii) the fluid was one dimensional plug flow; (iii) the fluid was laminar and Newtonian; (iv) the properties of the fluid and solid domains were constant and uniform; (v) thermal and mass diffusion were assumed to be negligible; (vi) transient response resulted from sudden change in the intensity of the incident solar radiation and/or inlet fluid temperature. This model is described by the following equations:

$$\frac{\partial\theta_s}{\partial\tau}=\frac{WSL\rho_f A_f}{T_\infty\rho_s A_s C_s m_f}-\frac{WL\rho_f A_f U_u}{\rho_s A_s C_s m_f}\theta_s-\frac{bL\rho_f A_f U_1}{\rho_s A_s C_s m_f}(\theta_s-\theta_f) \tag{90}$$

$$\frac{\partial\theta_f}{\partial\tau}+\frac{\partial\theta_f}{\partial X}=-\frac{dLU_s}{C_s m_f}\theta_f+\frac{bLU_1}{C_s m_f}(\theta_s-\theta_f) \tag{91}$$

where

$$\theta_f=\frac{(T_f-T_\infty)}{T_\infty},\qquad \theta_s=\frac{(T_s-T_\infty)}{T_\infty},\qquad \theta_0=\frac{(T_f(t,0)-T_\infty)}{T_\infty},$$
$$\tau=\frac{tm_f}{\rho_f A_f/L} \tag{92}$$

with the following initial and boundary conditions: $\theta_f(0,x)=\theta_s(0,x)=0$ and $\theta_f(\tau,0)=\theta_0(\tau)$.

The authors have outlined analytical solutions for the fluid and solid domains. The effects of different design parameters on the thermal performance of the heater were analyzed and the validity of the theoretical model was verified experimentally. It was found that both theoretical and experimental results were in good agreement.

Matrawy [49] proposed another mathematical model of this solar air heater design. The model was based on the following assumptions: (i) uniform temperature distribution across the width of absorber plate and of back plate; (ii) uniform distribution of the air flow along the collector channels; (iii) the physical properties of the flowing air was independent of temperature and pressure; (iv) only steady states were considered and the energy stored in the components was neglected; (v) all convective heat transfer coefficients between the collector components and flowing air were equal and constant through out the solution procedure (vi) the temperature of the flowing air was uniform over the collector cross-sectional area. The energy balance equations for the collector components were written as follows:

$$\text{For the absorber}:\quad U_t(T_p-T_a)+h_{cpf}(T_p-T_f)+h_{rpb}(T_p-T_b)$$
$$+\frac{1}{A_c}\left(-kAn\frac{dT_s}{dz}\right)_{z=0}=S \tag{93}$$

$$\text{For the plate}\quad h_{rpb}(T_p-T_b)+\frac{1}{A_c}\left(-Ank_s\frac{dT_s}{dz}\right)_{z=D}$$
$$=h_{cbf}(T_b-T_f)+U_b(T_b-T_a) \tag{94}$$

$$\text{For the metal slats}:\quad \left(-Ak_s\frac{dT_s}{dz}\right)_{z=0}-\left(-Ak_s\frac{dT_s}{dz}\right)_{z=D}$$
$$=\int_{z=0}^{z=D}2h_{csf}L_c(T_s-T_f)dz \tag{95}$$

$$\text{For the airflow}:\quad h_{cpf}(T_p-T_f)+h_{cbf}(T_b-T_f)$$
$$+\frac{1}{A_c}\int_{z=0}^{z=D}2h_{csf}nL_c(T_s-T_f)dz=q_u \tag{96}$$

where A_c is the collector total surface area (WLc) and A is the slat cross-sectional area (δLc). N is the number of metal vanes per meter of width. The determination of the radiative heat transfer was given in Duffie and Beckmann [52]. The convective heat transfer coefficients were computed on the basis of empirical correlations developed by Heaton et al. [21] and Nusselt [53] and given by Ong [7]. The solution of the above equations was carried out using an iterative procedure. It was concluded that the air collector with a box-type absorber can easily be modeled mathematically through the development of expressions for its parameters. The maximum number of metal vanes and depth of the air duct in a solar air collector are interesting factors for collector design.

The mathematical model proposed by Ammari [51] was similar to the above for the energy balance of the absorber plate, back (bottom) plate, slats metal (vanes) and air flow. For the cover Ammari [51] has proposed the follow:

$$h_{nc}(T_p-T_g)+h_{rpg}(T_p-T_g)=h_w(T_g-T_a)+h_{rga}(T_g-T_a) \tag{97}$$

The sky temperature is defined as [54]: $T_{sky}=0.0552T_a^{1.5}$. The flow is assumed to be hydro dynamically developed at the collector inlet.

Kabeel and Mecárik [50] have investigated a longitudinal fins collector with two covers. This model is show in Fig. 6c. By considering the energy balance for each part of the system in steady state heat flow were written as follow:

$$\text{For the top glass}: \quad \alpha_{g1}S + h_{rg1g2}(T_{g2} - T_{g1}) + h_{cg1a1}(T_{a1} - T_{g1}) - h_w(T_{g1} - T_a) = 0 \tag{98}$$

$$\text{For the air between the two glasses}: \quad h_{cg2a1}(T_{g2} - T_{a1}) + h_{cg1a1}(T_{g1} - T_{a1}) = 0 \tag{99}$$

$$\text{For the second glass cover}: \quad \tau_{g1}\alpha_{g2}S + h_{cg2f}(T_f - T_{g2}) + h_{rg2p}(T_p - T_{g2}) - h_{rg1g2}(T_{g2} - T_{g1}) - h_{cg2a1}(T_{g2} - T_{a1}) = 0 \tag{100}$$

$$\text{For absorber plate}: \quad \tau_{g1}\tau_{g2}\alpha_p S - Zh_{pf}(T_p - T_f) - h_{rpg2}(T_p - T_{g2}) - U_b(T_p - T_a) = 0 \tag{101}$$

Z is the ratio between the actual absorber area and the absorber area normal to the solar radiation falling upon the collector.

2.7. Two pass solar air heaters

The concept of a two-pass air heater was introduced by Satcunanathan and Deonarine [55] and later considered by Caouris et al. [56] for liquid based systems. These authors conducted experiments on the two-pass design with air flow between the two glass covers and under the absorber. Wijeysundera et al. [57] motivated by a need to consider in greater detail both analytically and experimentally the concept of two-pass design, developed heat transfer models for two-pass flow arrangements. In view of uncertainties which exist in the heat transfer coefficients for various processes, they are made the following assumptions to keep the analysis simpler: (i) The temperature, of the covers and absorber plate were uniform. (ii) For the thermally developing flow in a heater channel, suitably averaged heat transfer coefficients available in the literature were used. (iii) The bulk-mean temperature of the cooling fluid was changed only in the flow direction. (iv) The area of the collector was large compared to the thickness so that end losses and shading can be neglected. (v) Effects due to air leakage and temperature drop in the plenums were negligible. (vi) The absorber plate and the covers were diffuse-grey for long wave radiation. For incoming solar radiation the covers behave like specular reflectors. (vii) The collector was in quasi-steady state. Fig. 7 shows a schematic view of the two-pass flow arrangement under consideration. The air flows first between the covers and then through the bottom channel. There is a stagnant air gap between the absorber plate and the cover 2. For the various elements of the collector, Wijeysundera et al. [57] wrote the nodel energy equations as

$$\text{For cover 1}: \quad Q_{f1} = A_c\lambda_1 S + A_c h_{rg2g1}(T_{g2} - T_{g1}) - A_c(h_{g1a} + h_w)(T_{g1} - T_a) \tag{102}$$

$$\text{For cover 2}: \quad Q_{f2} = A_c\lambda_1 S - A_c h_{rg1g2}(T_{g2} - T_{g1}) + A_c(h_{rpg2} - h_{cpg2})(T_p - T_{g2}) \tag{103}$$

$$\text{For the absorber plate}: \quad Q_{pf} = A_c\lambda_p S - A_c h_{rpb}(T_p - T_b) - A_c(h_{rpg2} + h_{cpg2})(T_p - T_{g2}) \tag{104}$$

$$\text{For the bottom plate}: \quad Q_{bf} = A_c h_{rpb}(T_p - T_b) - A_c h_{cbf}(T_b - T_a) \tag{105}$$

$$\text{For the air flow between covers}: \quad Q_{f1} = A_c U_{21}\left[(T_2 - T_1) + F'(T_1 - T_{fi}) + F'\frac{h_{2f}}{h_{1f}}(T_2 - T_{fi})\right] \tag{106}$$

For the airflow between absorber plate and bottom plate :

$$Q_{f2} = A_c U_{21}\left[(T_{g2} - T_{g1}) + F'(T_{g1} - T_{fi}) + F'\frac{h_{cg1f}}{h_{cg2f}}(T_{g2} - T_{fi})\right] \tag{107}$$

with $F' = \dot{m}C/(h_{cg2f} + h_{cg1f})WL[1 - \exp(-(h_{cg2f} + h_{cg1f})WL/\dot{m}C)]$. Q is the total heat flux and the fractions λ_i of the solar radiation absorbed in the various elements of the collector are calculated using the net method [58]. A similar procedure has also been applied by Wijeysundera et al. [57] on the two-pass solar air heater with two covers. Wijeysundera et al. [57] used this mathematical model to study the thermal performance of the two-pass solar air heater design. The results show that the performance of the two-pass design with air flow above and below the absorber plate in turn is better than the single pass system. The results of the experiments and predictions of this heat transfer model have shown that there is some scatter in the experimental data. There results were also compared to the experimental data of Satcunanathan and Deonarine [55].

A new mathematical model has been proposed by Verma et al. [59]. They wrote down the energy balance equations for the design of Fig. 8 under usual assumptions [13] to show the optimization procedure used. The two-pass solar air heater design studied by Verma et al. [59] is different from the one modeled by Wijeysundera et al. [57] (see Figs. 7 and 8). These analyses give the following equations:

$$\text{At cover glazing}: \quad \alpha_g S = h_{rgs}(T_g - T_s) + h_{cgf1}(T_g - T_{f1}) + h_w(T_g - T_a) + h_{rgp}(T_g - T_p) \tag{108}$$

$$\text{At a fluid stream between cover and absorber}: \quad h_{cgf1}(T_g - T_{f1}) = h_{cf1p}(T_{f1} - T_p) + \frac{mC_f}{W}\frac{dT_{f1}}{dx} \tag{109}$$

$$\text{At absorber plate}: \quad \alpha_p\tau_g S + h_{rgp}(T_g - T_p) + h_{cf1p}(T_{f1} - T_p) = h_{cpf2}(T_p - T_{f2}) + h_{rpb}(T_p - T_b) \tag{110}$$

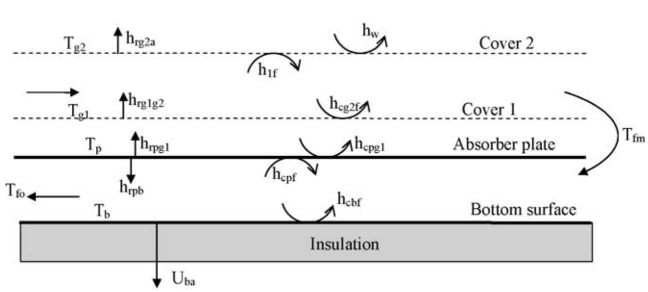


Fig. 7. Schematic view studied by Wijeysundera et al. [57].

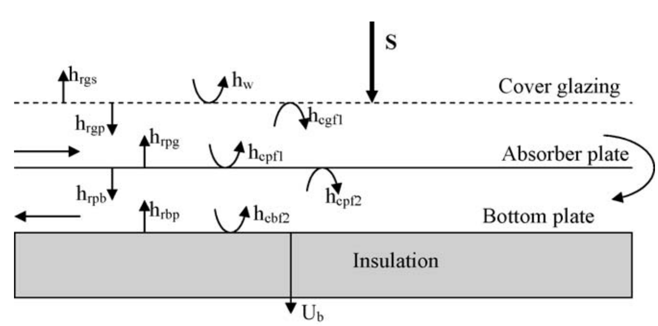


Fig. 8. Schematic view studied by Verma et al. [59].

At a fluid between absorber plate and a rear plate :

$$h_{cpf2}(T_p - T_{f2}) = h_{cf2b}(T_{f2} - T_b) + \frac{mC_f}{W}\frac{dT_{f2}}{dx} \quad (111)$$

At rear plate :

$$h_{cf2b}(T_{f2} - T_b) + h_{rpb}(T_p - T_b) = U_b(T_b - T_a) \quad (112)$$

The differential equations can be solved by using the following boundary conditions:

$$T_{f1}|_{x=0}T_{fi} \quad \text{and} \quad T_{f1}|_{x=L} = T_{f2}|_{x=L} \quad (113)$$

The temperature of the sky T_s have been calculated by using the expressions as given Swinbank [54]. An iterative procedure has been used by Verma et al. [59] to solve the above Eqs. (109)–(113). In this procedure, the temperatures of the cover, plate, air, etc. were initially assumed. The new temperatures were obtained by using the solution equations and were compared. The procedure was repeated until the solution is converged and finally the collector outlet air temperature was obtained. It was shown that there exists an optimum mass flow rate corresponding to an optimum flow depth.

The mathematical model proposed by Wijeysundera et al. [57] was used by Naphon and Kongtragool [17] to study numerically the effect of air mass flow rate on the heat transfer characteristic and performance of the single two-pass solar air heater. The explicit method of finite difference scheme was used to solve these models.

In order to study the effects of various design and operational parameters (duct length L, depths of inlet D_1, and outlet D_2 air flow channels and air mass flow rate) of the system, Choudhury et al. [33] modified a mathematical model proposed by Wijeysundera et al. [57]. The schematic view is identical to the one proposed by Verma et al. [59] (see Fig. 8). The steady-state energy balance equations for different plates and flowing air in the inlet and outlet channels of the air heaters, assuming the air inlet temperature to be the same as the ambient temperature, were written as follows [33]:

For the two-pass, single-cover air heater:

Cover glazing :

$$\alpha_g S = h_w(T_g - T_a) + h_{cgf1}(T_g - T_{f1}) + h_{rgp}(T_g - T_p) \quad (114)$$

Fluid between cover and absorber plate :

$$mC(T_{fo} - T_a) = h_{cgf1}(T_g - T_{f1}) + h_{cpf1}(T_p - T_{f1}) \quad (115)$$

Absorber plate :

$$\alpha_p \tau_g S = h_{cpf1}(T_p - T_{f1}) + h_{cpf2}(T_p - T_{f2}) + h_{rpb}(T_p - T_b) + h_{rpg}(T_p - T_g) \quad (116)$$

At a fluid between absorber plate and a rear plate :

$$mC(T_o - T_{fo}) = h_{cgf2}(T_p - T_{f2}) + h_{cbf2}(T_b - T_{f2}) \quad (117)$$

At rear plate :

$$h_{rpb}(T_p - T_b) - h_{cbf2}(T_p - T_{f2}) = U_b(T_b - T_a) \quad (118)$$

From the results discussed by these authors, it was concluded that the optimum values of the duct depths, which correspond to the minimum annual cost per unit solar energy gain, were different for different duct lengths and air mass flow rates.

Chauhan et al. [60] studying the drying characteristics of coriander in a stationary 0.5 tone/batch capacity deep-bed dryer coupled to a double-pass solar single air heater and a rock bed storage unit, proposed a new mathematical model for this air heater design (Fig. 8). The energy balance equations for different components of the solar air heater were given by the following:

At cover glazing :

$$M_g C_g \frac{dT_g}{dt} = \alpha_g S - h_{cgf1}(T_g - T_{f1}) - h_w(T_g - T_a) - h_{rgp}(T_g - T_p) \quad (119)$$

At a fluid stream between cover and absorber :

$$h_{cg1}(T_g - T_{f1}) - h_{cf1p}(T_{f1} - T_p) = \frac{mC_f}{W}\frac{dT_{f1}}{dx} + M_f C_f \frac{dT_{f1}}{dt} \quad (120)$$

At absorber plate :

$$\alpha_p \tau_g S + h_{rgp}(T_g - T_p) + h_{cf1p}(T_{f1} - T_p) - h_{cpf2}(T_p - T_{f2}) - h_{rpb}(T_p - T_b) = M_p C_p \frac{dT_p}{dt} \quad (121)$$

At a fluid between absorber plate and a rear plate :

$$h_{cpf2}(T_p - T_{f2}) - h_{cf2b}(T_{f2} - T_b) = \frac{mC_f}{W}\frac{dT_{f2}}{dx} + M_f C_f \frac{dT_{f2}}{dt} \quad (122)$$

At rear plate

$$h_{cf2b}(T_{f2} - T_b) + h_{rpb}(T_p - T_b) - U_b(T_b - T_a) = M_b C_b \frac{dT_b}{dt} \quad (123)$$

The initial and boundary conditions were: $T_{f1}(x,0) = T_a(1)$, $T_{f2}(x,0) = T_a(1)$, $T_p(x,0) = T_b(x,0) = T_g(x,0) = T_a(1)$, $T_{f1}(0,t) = T_a = T_{fi}$, $T_{f1}(L,t) = T_{f2}(0,t)$, $T_{f2}(L,t) = T_{fo}$.

Choudhury at al. [33] have investigated a double pass solar air heater with double cover. This model is shown in Fig. 9. It consists of double covers, double channel design with double air flows between inner cover and absorber plate and between absorber and bottom plates and with insulation provided. The mathematical model proposed by these authors is as follows:

Cover 2 :

$$\alpha_{g2} S = h_w(T_{g2} - T_a) + h_{cg2g1}(T_{g2} - T_{g1}) + h_{rg2g1}(T_{g2} - T_{g1}) \quad (124)$$

Cover 1 :

$$\alpha_{g1} \tau_{g2} S = h_{rg2g1}(T_{g1} - T_{g2}) + h_{cg2g1}(T_{g1} - T_{g2}) + h_{cg2f1}(T_{g1} - T_{f1}) + h_{rpg1}(T_{g1} - T_p) \quad (125)$$

Fluid between absorber plate and a cover 2 :

$$mC(T_{f1o} - T_a) = h_{cg1f1}(T_{g1} - T_{f1}) + h_{cpf1}(T_p - T_{f1}) \quad (126)$$

Absorber plate :

$$\alpha_p \tau_{g2} \tau_{g1} S = h_{rpg1}(T_p - T_{g1}) + h_{cpf1}(T_p - T_{f1}) + h_{cpf2}(T_p - T_{f2}) + h_{rpb}(T_p - T_b) \quad (127)$$

At a fluid between absorber plate and a rear plate :

$$mC(T_{f2o} - T_{f1o}) = h_{cgf2}(T_p - T_{f2}) + h_{cbf2}(T_b - T_{f2}) \quad (128)$$

At rear plate

$$h_{rpb}(T_{f2o} - T_b) - h_{cbf2}(T_b - T_{f2}) = U_b(T_b - T_a) \quad (129)$$

Choudhury et al. [33] has not taken account of the heat transfer by the radiation from the cover to the sky. In the above equations T_{f1} and T_{f2} are given by: $T_{f1} = (T_{f1o} + T_a)/2$ and $T_{f2} = (T_{f2o} + T_{fo})/2$. The various heat transfer coefficients used in this analysis have been computed by using the equations given in Duffie and Beckann [5], Tan and Charters [6] and Hollands et al. [61] (see Table 1).

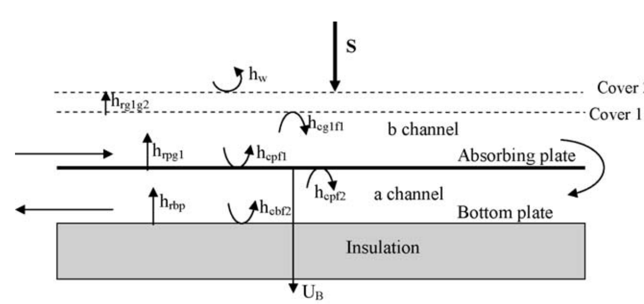


Fig. 9. Schematic view of energy-flow of double-pass type solar air heater (see Choudhury et al. [33]).

Recently, to evaluate the effects of two kinds of roof solar collector, Zhai et al. [18] used the mathematical model developed by Choudhury et al. [33]. In this work, for the natural ventilation mode, the mean air temperatures in each channel were calculated according to Hirunlabh et al. [62].

$$T_{fm} = 0.75\,T_{2o} + 0.25\,T_r \tag{130}$$

and the air mass flow rate per unit of the system was given by

$$m_{fi} = \rho \frac{A_{in}}{A_{p1}} \sqrt{\frac{2gL\sin(\beta)(T_{io} - T_r)}{T_r(\xi_{in} + \xi_o + f\frac{L}{D})}} \tag{131}$$

with $\xi_{in} = 1.5$, $\xi_0 = 1.0$, $f = 0.056$. The results show that the double pass roof solar collector is more efficient.

Recently Yamali and Solmus [63] have investigated a desalination system which has a double-pass flat plate solar air heater with two covers as a component. In their work, a transient analysis of double-pass solar air heater has been carried out. The energy balance equations are follows:

$$\text{For cover 2}: \quad M_g C_g \frac{dT_{g2}}{dt} = \alpha_g SWL + WL\,h_{rg1g2}(T_{g1} - T_{g2}) - WL\,h_w(T_{g2} - T_a) - WL\,h_{rg2sky}(T_{g2} - T_{sky}) + WL\,h_{cg1g2}(T_{g1} - T_{g2}) \tag{132a}$$

with

$$T_{sky} = T_a - 6 \tag{132b}$$

$$\textit{For cover 1}: \; M_g C_g \frac{dT_{g1}}{dt} = \alpha_g \tau_g SWL_c + WL\,h_{rpg1}(T_p - T_{g1}) - WL\,h_{cg1f1}(T_{g1} - T_{f1}) - WL\,h_{cg1g2}(T_{g1} - T_{g2}) - WL\,h_{cg1g2}(T_{g1} - T_{g2}) \tag{133}$$

$$\text{First air pass}: \quad M_f C_f \frac{dT_{f1}}{dt} = WLh_{cpf1}(T_p - T_{f1}) + WLh_{cg1f1}(T_{g1} - T_{f1}) - m_f C_f(T_{f1o} - T_{f1i}) \tag{134}$$

$$\text{Absorber plate}: \quad M_g C_g \frac{dT_{g1}}{dt} = \alpha_g \tau_g^2 SWL_c - WLh_{cpf2}(T_p - T_{f2}) - WLh_{cpf1}(T_p - T_{f1}) - WLh_{rpg1}(T_p - T_{g1}) - WLh_{rpb}(T_p - T_b) \tag{135}$$

$$\text{Second air pass}: \quad M_f C_f \frac{dT_{f2}}{dt} = WLh_{cpf2}(T_p - T_{f2}) + WLh_{cbf2}(T_b - T_{f2}) - m_f C_f(T_{f2o} - T_{f1o}) \tag{136}$$

The four order Runge–Kutta method was used to solve numerically the energy balance equations. For this purpose, a computer simulation program based on mathematical model was developed by means of MATLAB software. Theoretical results illustrated that the system productivity is strongly affected by the solar air heater area and slightly influenced by the wind speed variations and bottom heat loss coefficients of the solar air heater.

With the aim to reduce losses from the front cover of the collector, Mohamad [15] modified the two-pass solar air heater with two cover proposed by Choudhury et al. [33] and Wijeysundera et al. [57]. The schematic view is shown in Fig. 10. This model consists of double covers, double channel design with double air flows between upper cover and inner cover and between inner cover and absorber plate, the lower surface of the absorber is in contact of the insulation provided. Under steady state operating conditions, he has written the energy balances for this design as follows:

$$\text{Cover 2}: \quad \alpha_{g2} S = h_w(T_{g2} - T_a) + h_{cg2f1}(T_{g1} - T_{f1}) + h_{rg1g2}(T_{g2} - T_{g1}) \tag{137}$$

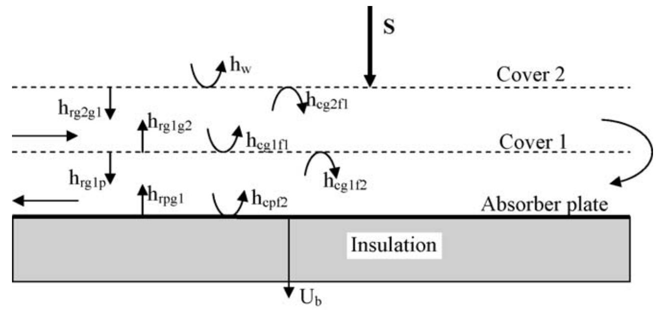


Fig. 10. Schematic view studied by Mohamad [15].

$$\text{Fluid between the covers}: \quad h_{cgf1}(T_{g2} - T_{f1}) + h_{cf1g1}(T_{f1} - T_{g1}) = \frac{mC_f}{W}\frac{dT_{f1}}{dx} \tag{138}$$

$$\text{Cover 1}: \quad \alpha_{g1}\tau_{g2} S = h_{rg2g1}(T_{g1} - T_{g2}) + h_{cg1f1}(T_{g1} - T_{f1}) + h_{cf2g1}(T_{g1} - T_{f2}) + h_{rg1p}(T_{g1} - T_p) \tag{139}$$

Fluid between the cover 2 and the absorber plate :

$$h_{cf2g1}(T_{g1} - T_{f2}) + h_{cf2p}(T_p - T_{f2}) = \frac{mC_f}{W}\frac{dT_{f2}}{dx} \tag{140}$$

$$\text{For the absorber plate}: \quad \alpha_p \tau_{g2} \tau_{g1} S = h_{cf2p}(T_p - T_{f2}) + h_{rpg1}(T_p - T_{g1}) + U_b(T_p - T_a) \tag{141}$$

In order to increase heat transfer from the absorber to the air, Mohamad [15] suggested replacing the absorber plate by a porous matrix absorber. In this case, if it was assumed that the air and the solid matrix were in thermal equilibrium (the temperature of solid was equal to the temperature of the air locally), the energy balance in the second passage can be simplified as

$$h_{f2g1}(T_{g1} - T_{f2}) + U_a(T_a - T_{f2}) + k_{eff}\frac{d^2T_{f2}}{dx^2} + \alpha_p \tau_{g1}\tau_{g2} S = \frac{mC_f}{W}\frac{dT_{f2}}{dx} \tag{142}$$

The results indicate that, under normal operating conditions, the thermal efficiency of the suggested heater is much higher than the efficiency of the conventional air heaters.

2.8. Double-pass flat-plate solar air heater with recycle

Recently, it was reported that increasing the fluid velocity by using recycle in double-pass parallel-plate heat exchangers enhances the heat-transfer coefficient, resulting in improved performance [65]. The schematic view of the design of the solar heater is shown in Fig. 11. In addition to increasing the fluid velocity, the recycle operation also produces an effect by remixing the inlet fluid with the hot outgoing fluid. Due to the fact that the strength of forced heat convection by using recycle effects plays an important role in designing and operating the solar air heaters, Ho et al. [66] developed the mathematical formulation for a double-pass solar air heater with recycle. In this model, the following assumptions were made: the temperatures of the absorbing plate, bottom plate and bulk fluid are functions of the flow direction only. Both glass covers and fluids do not absorb radiant energy. The radiant energy absorbed by the outlet cover is assumed to be negligible [66]. With the

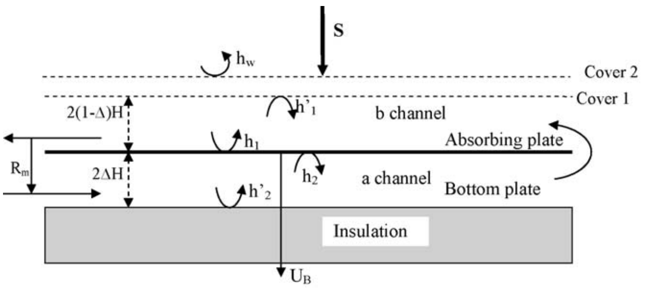


Fig. 11. Schematic view of energy-flow of double-pass type solar air heater with recycle (see Ho et al. [66]).

above assumptions, the energy equations were written as follows:

$$\text{Cover 1}: \quad h_{rpg2}(T_p - T_{g1}) + h'_1(T_b(z) - T_{g1}) = U_{g1s}(T_{g1} - T_s) \tag{143}$$

$$\text{Absorbing plate}: \quad \alpha_p \tau_{g1} \tau_{g2} S - h_T(T_p - T_s) + h_B(T_p - T_s) + h_1(T_p - T_b(x)) + h_2(T_p - T_a(x)) \tag{144}$$

$$\text{Bottom plate}: \quad h_{rpR}(T_p - T_R) + h'_2(T_a(x) - T_R) = U_{B1s}(T_p - T_s) \tag{145}$$

$$\text{Channel a}: \quad h_2(T_p - T_a(x)) - h'_2(T_a(x) - T_R) = \left[\frac{(R+1)mC_p}{W}\right] \frac{dT_a(x)}{dx} \tag{146}$$

$$\text{Channel b}: \quad h_1(T_p - T_b(x)) - h'_1(T_b(x) - T_{g1}) = \left[\frac{-(R+1)mC_p}{W}\right] \frac{dT_b(x)}{dx} \tag{147}$$

In this equation, the characteristic length is the equivalent diameter of the duct. For the open conduit, lower channel and upper channel, they are respectively given by:

$$D_{e,o} = \frac{4HW}{2H + W}, \qquad D_{e,a} = \frac{(4\Delta H)W}{(2\Delta H) + W} \quad \text{and} \quad D_{e,a} = \frac{[4(1-\Delta)H]W}{[2(1-\Delta)H] + W} \tag{148}$$

and the air velocities of the open conduit, lower channel and upper channel used by Ho et al. [66] are given by

$$\bar{v}_o = \frac{m}{(2HW)\rho}, \qquad \bar{v}_a = \frac{(1+R)m}{(2\Delta H)W\rho} \quad \text{and} \quad \bar{v}_b = \frac{[m(1+R)]}{[2(1-\Delta)H]W\rho} \tag{149}$$

Δ is the ration of channel thickness.

The experiment had been carried out by these authors. With an iterative procedure, Ho et al. [66] investigated the effect on the collector efficiency with ratio as the variable parameter for this type of solar air heater design (see Fig. 11). The results showed that the theoretical prediction agree reasonably well with experimental data. It was also confirmed that the collector modules with external recycle are thermo-hydraulically better. This is economically feasible in the design of double-pass flat solar air heaters.

2.9. Double-pass flat plate solar air heater with porous media

Naphon [69] studied theoretically the heat transfer characteristics and performance of double-pass flat solar air heater with and without porous media. The model was based on that of Naphon and Kongtragool [17] with the following assumption: (i) flow of air is steady, (ii) outside convective heat transfer coefficient is constant along the length of solar air heater, (iii) inside convective heat transfer coefficient is constant along the length of solar air heater, (iv) thermal conductivity of porous media is constant along the length of solar air heater.

The mathematical model proposed in this study for the design of the double-pass single solar air collector with porous media is based on the one proposed by Naphon and Kongtragool [17] and Wijeysundera et al. [57]. The equations of the top glass cover, the first-pass air, the absorber plate and the bottom plate are similar to given by Eqs. (108), (110) and (112). With the presence of the porous media in the second-pass air, heat transfer Eq. (111) becomes:

$$mC_p \frac{dT_{f2}}{dx} = K_p \frac{d^2 T_{f2}}{dx} + h_{cf2p}(T_p - T_{f2}) + h_{cf2b}(T_b - T_{f2}) \tag{150}$$

k_p is the thermal conductivity of the porous media. The implicit method of finite-difference scheme had been employed to solve these models. The effect of the thermal conductivity of the porous media on the heat transfer characteristics and performance have been considered. The theoretical results obtained from the model were validated by comparison with the experimental data of Sopain et al. [70] and there was reasonable agreement.

2.10. Double-pass flat plate solar air heater with longitudinal fins

Naphon [71] has investigated heat transfer characteristics and entropy generation of the double-pass flat plate solar air heater with longitudinal fins. The basic physical equations used to describe the heat transfer characteristics of the solar air heater, as shown in Fig. 12a and b, are developed from the conservation equations of energy.

With the first law of thermodynamics and based on the Naphon and Kongtragood's model [17], Naphon developed a mathematical model for double-pass flat solar air heater with longitudinal fins. Using the assumption proposed in the case of double pass solar air heater with porous media, the following equations have been developed:

$$\text{For the glass cover}: \quad \alpha_g S = h_w(T_g - T_a) + h_{cf1cg}(T_g - T_{f1}) + h_{rgp}(T_g - T_p) + h_{rag}(T_g - T_a) \tag{151}$$

$$\text{For the first-pass air}: \quad mC_f \frac{dT_{f1}}{dx} = h_{cf1g}(T_g - T_{f1}) + h_{cf1p}(T_p - T_{f1}) + \frac{N}{A_{\text{frontal}}} \int_{z=0}^{z=H} 2Lh_1(T_{v1} - T_{f1})dz \tag{152}$$

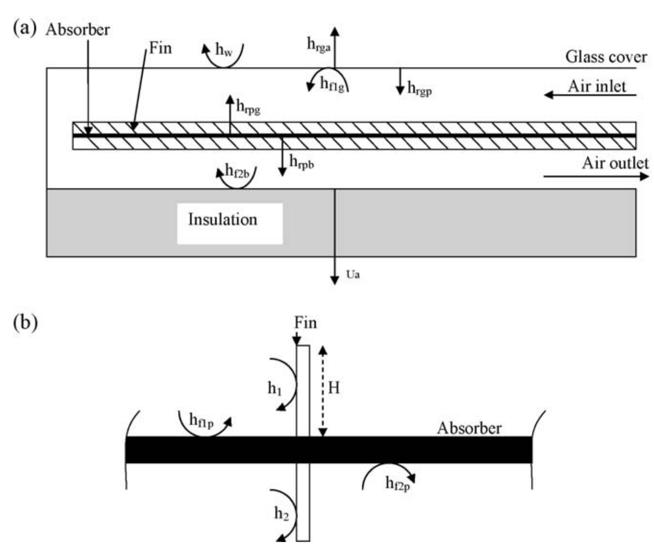


Fig. 12. (a) Schematic diagram of the solar heater (Naphon [71] model). (b) Schematic diagram of fin section (Naphon [71] model).

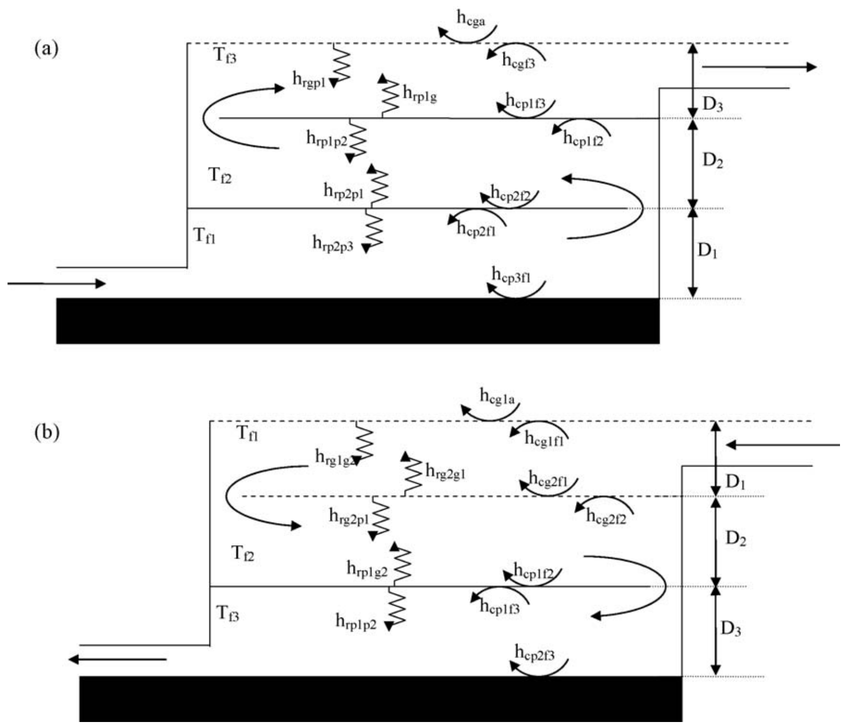


Fig. 13. (a) Three pass single cover air heater (Chandra et al. [72]). (b) Three pass two covers air heater (Choudhury et al. [75]).

where m is the mass flow rate of fluid per unit with, $A_{frontal}$ is the frontal area of the channel, H is the height of the fin, z is the distance from the absorber plate, T_{v1} is the fin temperature in the upper channel and L is the length of the collector. N is the number of fins.

$$\text{For the upper fin :}\quad \frac{N}{A_{frontal}}\int_{z=0}^{z=H} 2Lh_1(T_{v1}-T_{f1})dz = \frac{N}{A_{frontal}}\left(-kA\frac{dT_{v1}}{dz}\right)_{z=0} \tag{153}$$

$$\text{For absorber plate :}\quad \alpha_g\tau_g S = h_{cf1p}(T_p-T_{f1}) + h_{cf2p}(T_p-T_{f2}) + h_{rgp}(T_p-T_g) + h_{rpb}(T_p-T_b) + \frac{N}{A_{frontal}}\left[\left(-kA_{sf}\frac{dT_{v1}}{dz}\right)_{z=0} + \left(-kA_{sf}\frac{dT_{v2}}{dz}\right)\right] \tag{154}$$

T_{v2} is the fin temperature in lower channel and A_{sf} is the cross-section area of fin.

$$\text{For lower fin :}\quad \frac{N}{A_{frontal}}\int_{z=0}^{z=H} 2Lh_2(T_{v2}-T_{f2})dz = \frac{N}{A_{frontal}}\left(-kA\frac{dT_{v2}}{dz}\right)_{z=0} \tag{155}$$

$$\text{For second-pass air :}\quad mC_f\frac{dT_{f2}}{dx} = h_{cf2p}(T_p-T_{f2}) + h_{cf2p}(T_p-T_{f2}) + \frac{N}{A_{frontal}}\int_{z=0}^{z=H} 2Lh_2(T_{v2}-T_{f2})dz \tag{156}$$

$$\text{For bottom plate :}\quad h_{cf2b}(T_b-T_{f2}) + h_{rpb}(T_p-T_b) + U_a(T_b-T_a) = 0 \tag{157}$$

It was found that the thermal efficiency increases with increasing the height and number of fins.

2.11. Triple pass solar air heaters

The schematic configuration of a typical triple-pass solar air heater is shown in Fig. 13a. It consists of one cover, an absorber plate and two rear plates (Fig. 13a). Chandra et al. [72] have investigated this design. Neglecting the thermal capacity of the plates, the energy balance equations were written as follows:

$$\text{Cover :}\quad \alpha_g S = h_{rgs}(T_g-T_s) + h_w(T_g-T_a) + h_{cgf3}(T_g-T_{f3}) + h_{rgp1}(T_g-T_{f3}) \tag{158}$$

$$\text{Fluid 3 :}\quad \frac{mC_f}{W}\frac{dT_{f3}}{dx} = h_{cgf3}(T_g-T_{f3}) - h_{cp1f3}(T_{f3}-T_{p1}) \tag{159}$$

$$\text{Plate 1 :}\quad \tau_g\alpha_{p1}S = h_{rgp1}(T_g-T_{p1}) + h_{cp1f3}(T_{p1}-T_{f3}) + h_{rp1r2}(T_{p1}-T_{p2}) + h_{cp1f2}(T_{p1}-T_{f2}) \tag{160}$$

$$\text{Fluid 2 :}\quad \frac{-mC_f}{W}\frac{dT_{f2}}{dx} = h_{cp1f2}(T_{p1}-T_{f2}) - h_{cp2f2}(T_{f2}-T_{p2}) \tag{161}$$

$$\text{Plate 2 :}\quad h_{rp1p2}(T_{p1}-T_{p2}) + h_{cf2p2}(T_{f2}-T_{p2}) = h_{rp2b}(T_{p2}-T_b) + h_{cp2f1}(T_{p2}-T_{f1}) \tag{162}$$

$$\text{Fluid 1 :}\quad \frac{mC_f}{W}\frac{dT_{f1}}{dx} = h_{cpf1}(T_{p2}-T_{f1}) - h_{cbf1}(T_{f1}-T_b) \tag{163}$$

$$\text{Plate 3 :}\quad h_{rp2b}(T_{p2}-T_{p3}) + h_{cbf1}(T_{f1}-T_b) = U_r(T_b-T_a) \tag{164}$$

with $T_{f1}(x=0)=T_a$, $T_{f1}(x=L)=T_{f2}(L)$ and $T_{f2}(0)=T_{f3}(0)$.

In order to appreciate the analytical results, numerical calculations have been carried out corresponding to the experi-

mental data of Ezeike [74]. The results of this theoretical work differ substantially from Ezeike's results. The results obtained from an exact analysis and from an approximate equivalent thermal network method were almost consistent.

This model of solar air heater has also been investigated by Choudhury et al. [75]. They assumed that the air inlet temperature is the same as the ambient temperature. In the mathematical model proposed by these authors, Eq. (158) is reconsidered without the term of radiative exchange between the cover and the sky; Eqs. (160), (162) and (163) are the same. Eqs. (159), (161) and (163) have been replaced by the following:

$$\text{Fluid 3}: \quad mC_f(T_{fo} - T_{f2o}) = h_{cg\,f3}(T_g - T_{f3}) - h_{cp1\,f3}(T_{f3} - T_{p1}) \tag{165}$$

$$\text{Fluid 2}: \quad mC_f(T_{f2o} - T_{f1o}) = h_{cp1\,f2}(T_{p1} - T_{f2}) - h_{cp2\,f2}(T_{f2} - T_{p2}) \tag{166}$$

$$\text{Fluid 1}: \quad mC_f(T_{f1o} - T_a) = h_{cp2\,f1}(T_{p2} - T_{f1}) - h_{cp3\,f1}(T_{f1} - T_{p3}) \tag{167}$$

Another three-pass solar air heater was investigated by Choudhury et al. [75]. It consists of two covers, an absorber and a rear plate (Fig. 13b). Assuming the air inlet temperature to be the same as the ambient temperature, the steady state energy balance equations for the different plates and flowing air in the inlet, intermediate and outlet channels of the air heaters can be written as follows:

$$\text{Cover 1}: \quad \alpha_{g1}S = h_{g1a}(T_{g1} - T_a) + h_{rg2g1}(T_{g1} - T_{g2}) + h_{cg1\,f1}(T_{g1} - T_{f1}) \tag{168}$$

$$\text{Fluid 1}: \quad mC_f(T_{f1o} - T_a) = h_{cg1\,f1}(T_{g1} - T_{f1}) - h_{cg2\,f1}(T_{g2} - T_{f1}) \tag{169}$$

$$\text{Cover 2}: \quad \tau_{g1}\alpha_{p2}S = h_{cg2\,f1}(T_{g2} - T_{f1}) + h_{cg2\,f2}(T_{g2} - T_{f2}) + h_{rg2g1}(T_{g2} - T_{g1}) + h_{rp1\,p2}(T_{p1} - T_{p2}) \tag{170}$$

$$\text{Fluid 2}: \quad \dot{m}C(T_{f2o} - T_{f1o}) = h_{cg2\,f2}(T_{g2} - T_{f2}) - h_{cp1\,f2}(T_{p1} - T_{f2}) \tag{171}$$

$$\text{Absorber}: \quad \tau_{g1}\tau_{g2}\alpha_{p1}S = h_{cp1\,f2}(T_{p1} - T_{f2}) + h_{cp1\,f3}(T_{p1} - T_{f3}) + h_{rp1g2}(T_{p1} - T_{g2}) + h_{rp1\,p2}(T_{p1} - T_{p2}) \tag{172}$$

$$\text{Fluid 3}: \quad mC_f(T_{fo} - T_a) = h_{cp1\,f3}(T_{p1} - T_{f3}) - h_{cp2\,f3}(T_{f3} - T_{p2}) \tag{173}$$

$$\text{Rear plate}: \quad h_{rp1\,p2}(T_{p1} - T_{p2}) + h_{cp2\,f3}(T_{f3} - T_{p2}) = U_r(T_{p2} - T_a) \tag{174}$$

In all these equations T_{f1}, T_{f2} and T_{f3} are defined as $T_{f1} = (T_{f1o} + T_a)/2$, $T_{f2} = (T_{f2o} + T_{f1o})/2$ and $T_{f3} = (T_{fo} + T_{f2o})/2$, respectively. In this study, the authors have made an effort to find the effects of duct length, duct depths of inlet (D_1), intermediate (D_2) and outlet (D_3) air channel and mass flow rate (m) on the cost benefit ratio. Efforts were also made to identify the most superior air heater by comparing the cost effective performance of these air heaters with those of single pass with no, single and double cover and two pass with single and double covers air heaters studied earlier by the authors [33,75]. Choudhury et al. [75] in their analysis have used the heat transfer coefficients predicted by the equations given in Duffie and Beckmann [5], Tan and Charter [6] and Hollands and Shewen [61]. It was shown that the double cover, three pass solar air heater with air flow from top to bottom is observed to be more cost-effective than the single cover, three pass solar air heater with air flow from bottom to top.

2.12. Multi-pass flat-plate solar air heaters with external recycle

Ho et al. [76] have developed a theoretical formulation for a multi-pass solar air heater with external recycle and investigate the recycle effect on collector efficiency. The effects of channel thickness ratio on the collector efficiency was also studied. In this study, Ho et al. [76] have considered a recycled four-pass solar air heater with vertical thickness $2\alpha H$ and $2(1-\alpha)H$ (α is the channel thickness ratio in vertical direction), and horizontal width $2\beta H$ and $2(1-\beta)H$ (β is the channel thickness ratio in horizontal direction), respectively, which was obtained by inserting an absorbing plate and insulation sheet with negligible thickness into a parallel

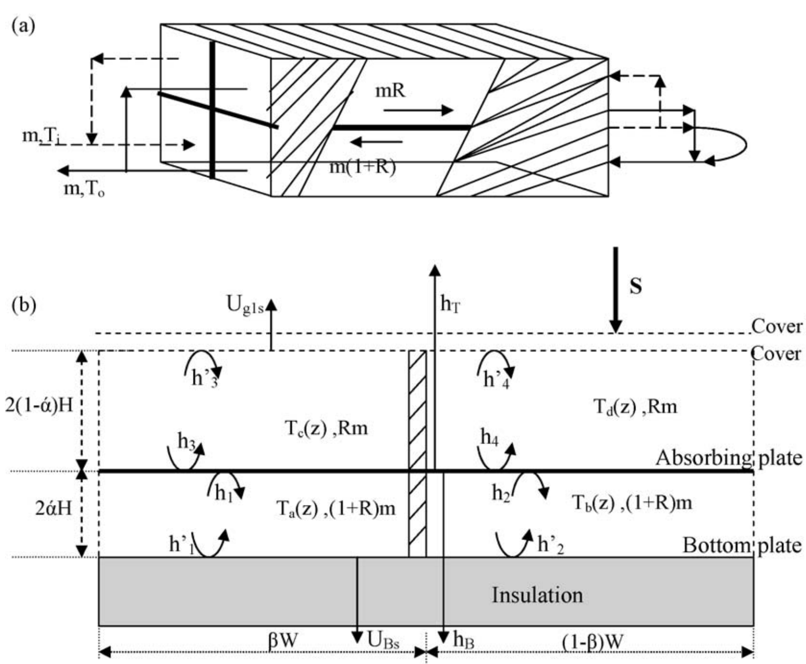


Fig. 14. (a) Multi-pass flat-plate solar air heater with recycle (Ho et al. [76]). (b) Schematic view of energy-flow of multi-pass type solar air heater with recycle (see Ho et al. [76]).

conduit of height 2H, length L, and width W (see Fig. 14). Assuming that: (i) the temperatures of the absorbing plate, bottom plate and bulk fluid were functions of the flow direction only, (ii) both glass covers and fluids do not absorb radiant energy, (iii) the absorptance of the glass cover 2 was negligible, the energy equations have been written as

$$\text{Cover 1}: \quad h_{rpg1}(T_p - T_{g1}) + h'_3(T_c(x) - T_{g1}) + h'_4(T_d(x) - T_{g1}) = U_{gls}(T_{g1} - T_s) \tag{175}$$

$$\text{Absorbing plate}: \quad \alpha_p \tau_{g1} \tau_{g2} S - h_T(T_p - T_s) - h_B(T_p - T_s) - h_1(T_p - T_a(x)) - h_2(T_p - T_b(x)) + h_3(T_c(x) - T_p) + h_4(T_d(x) - T_p) = 0 \tag{176}$$

$$\text{Bottom plate}: \quad h'_1(T_a(x) - T_R) + h'_2(T_b(x) - T_R) + h_{rpR}(T_p - T_R) = U_{Bs}(T_p - T_s) \tag{177}$$

Channel a(flowing under the absorber plate) :

$$h_1(T_p - T_a(x)) - h'_1(T_a(x) - T_R) = \left[\frac{(R+1)mC_p}{W\beta}\right]\frac{dT_a(x)}{dx} \tag{178}$$

$$\text{Channel b}: \quad h_2(T_p - T_b(x)) - h'_2(T_b(x) - T_R) = \left[\frac{-(R+1)mC_p}{(1-\beta)W}\right]\frac{dT_b(x)}{dx} \tag{179}$$

$$\text{Channel c}: \quad h_3(T_p - T_c(x)) - h'_3(T_c(x) - T_{g1}) = \left[\frac{-RmC_p}{W\beta}\right]\frac{dT_b(x)}{dx} \tag{180}$$

$$\text{Channel d}: \quad h_4(T_p - T_d(x)) - h'_4(T_d(x) - T_{g1}) = \left[\frac{RmC_p}{(1-\beta)W}\right]\frac{dT_b(x)}{dx} \tag{181}$$

In this work, the equivalent diameters were defined as

$$D_{e,a} = \frac{(4\alpha H)W\beta}{(2\alpha H) + W\beta}, \qquad D_{e,b} = \frac{[4\alpha H]W(1-\beta)}{[2\alpha H] + W(1-\beta)}, \qquad D_{e,c} = \frac{[4(1-\alpha)H]W\beta}{[2(1-\alpha)H] + W\beta}, \qquad D_{e,d} = \frac{[4(1-\alpha)H]W(1-\beta)}{[2(1-\alpha)H] + W(1-\beta)} \tag{182}$$

and average air velocities given by the following:

$$\bar{v}_a = \frac{m_a}{(2\alpha H)W\beta\rho}, \qquad \bar{v}_b = \frac{m_b}{2H\alpha W(1-\beta)\rho}, \qquad \bar{v}_c = \frac{m_c}{2H(1-\alpha)W\beta\rho}, \qquad \bar{v}_d = \frac{m_d}{2H(1-\alpha)W(1-\beta)\rho} \tag{183}$$

The above set of equations was solved numerically using an iterative procedure. In this procedure, the prescribed collector geometries, system properties and operating conditions were given, as well the initial guesses of the mean temperatures were specified for calculating the physical properties. The new values of mean temperatures were then re-calculated. If the re-calculated average temperature values were not quite close to the assumed values, the iteration calculations performed above will be done until the last assumed values meet the final calculated values. The results have shown that, the introduction of recycle effect was a feasible way to increase the collector coefficient due to the increasing fluid velocity effect and may compensate for the temperature difference decrement.

2.13. Solar air heater with a compound parabolic concentrator

Fig. 15 shows this solar air model. Pramuang and Exell [77] reported the results of an experimental study in which the method of Chungpaibulpatana and Exell is used to determine the collector parameters of a solar flat plate collector with a CPC for heating air. Recently, Tchinda [78] has quantified the heat transfer within this design of solar air heater and a mathematical model analysing the collector thermal performance has been proposed. In this model (see Fig. 15), the following assumptions were made: (i) It was assumed that the CPC is ideal and free from fabrication errors. (ii) Any beam of radiation incident within the acceptance angle θ_a, with the help of the parabolic reflector can reach the receiver. (iii) The reflection of radiation from the parabolic reflector was accounted for by the apparent reflectance $\rho_m^{<n>}$. (iv) The direction of the beam radiation incident on various components in the collector can be found though geometry. (v) The succeeding absorption and transmission processes inside CPC were diffusive and were accounted for in terms of diffuse properties. The solar and infrared energy exchanges in the collector were treated separately using pertinent radiative properties in the spectrum. (vi) Physical and optical properties of materials were assumed to be independent of temperature. (vii) The concentrator did not produce an image of the light source; hence it was called non-imaging concentrators. With the above assumptions, the energy equations may be written as follows:

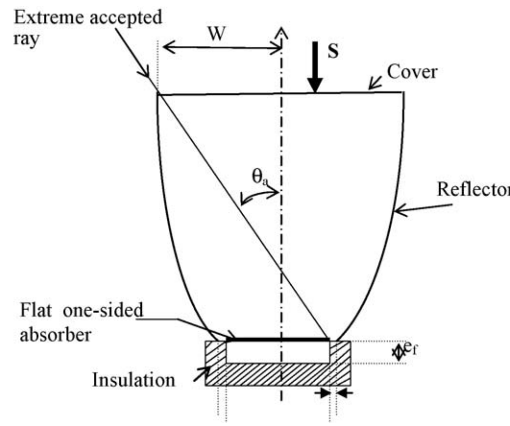


Fig. 15. Schematic view of a solar air heater with a compound parabolic concentrator (Premuang and Exell [77] and Tchinda [78]).

$$\text{For cover}: \quad M_c M_{pc}\frac{\partial T_c}{\partial t} = I(t)[\bar{\alpha}_c + \bar{\alpha}_c\bar{\tau}_c\bar{\rho}_p\rho_m^{2\langle n\rangle}]\frac{A_c}{A_p} + h_{Rp}(T_p - T_c) + h_{p/c}(T_p - T_c) - h_{Rs}(T_c - T_s) - h_{c/a}(T_c - T_b) \tag{184}$$

with $t > 0$.

$$\text{For plate absorber}: \quad M_p C_{pp}\frac{\partial T_p}{\partial t} = I(t)\bar{\tau}_c\rho_m^{\langle n\rangle}P\left[\bar{\alpha}_p + \bar{\alpha}_p\bar{\rho}_p\bar{\rho}_c\frac{A_p}{A_c}\right]\frac{A_c}{A_p} - h_{Rp}(T_p - T_c) - h_{p/c}(T_p - T_c) - q_u(t) \tag{185}$$

with t > 0.

$$\text{For fluid}: \quad \rho_f e_f C_{pf}\frac{\partial T_f}{\partial t} = q_u(t) - \frac{mC_{pf}}{l_p}\frac{\partial T_f}{\partial x} - U_0(T_f - T_b) \tag{186}$$

with $t > 0$ and $0 < x < L$. where $P = 1 - g/l_p$ ([80]), g is the gap thickness. $A_c = W^*L$, $A_p = l_p{}^*L$ and $q_u = U_f(T_p - T_f)$. An iterative method was used by the author to bring the effect of the temperature dependence of various heat transfer coefficients. For certain temperatures, they were first calculated by using the standard expressions given earlier. Equations were solved by assuming the constant and the new solutions used to generate all

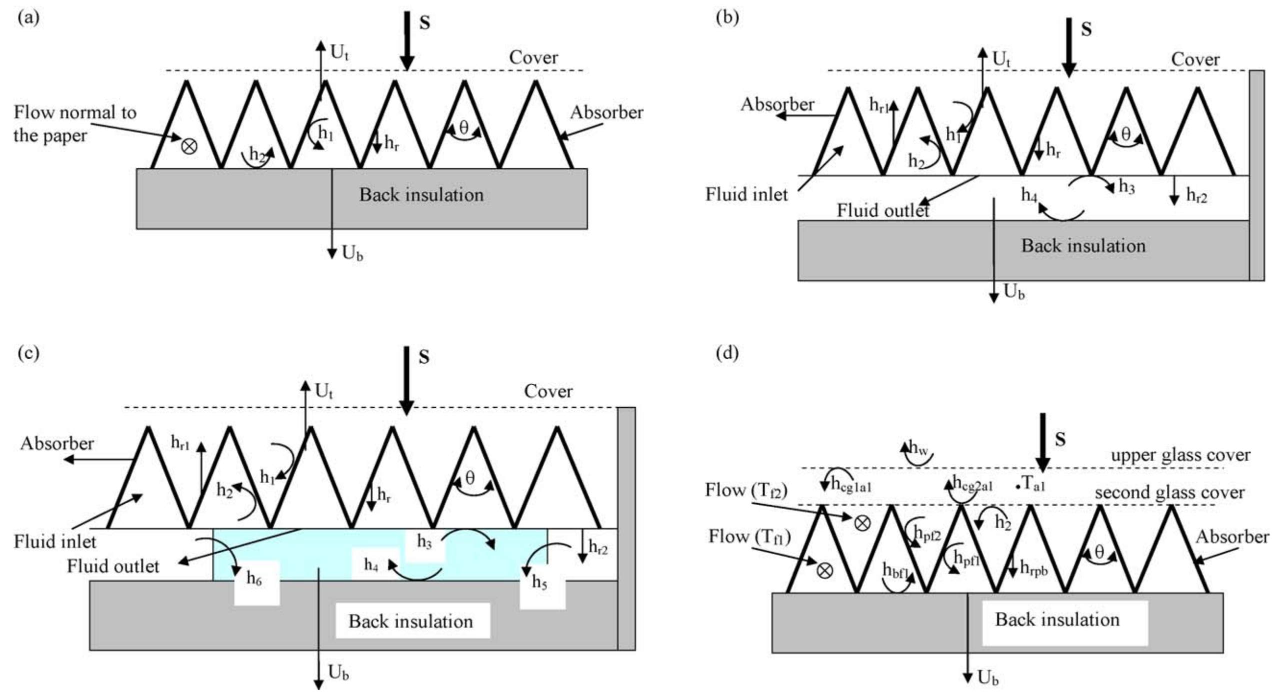


Fig. 16. (a) v-Groove air collector, Karim and Hawlader [83]. (b) v-Groove air collector (Bashria et al. [84]). (c) v-Groove air collector with porous media (Bashria et al. [85]). (d) v-Groove air collector (Kabeel and Mecarik [50]).

the heat transfer coefficients again till the values converge. This model has been validated with the experimental data of Pramuang and Exell [77].

2.14. V-groove solar air collector

The design given in Fig. 16a was also studied experimentally and theoretically by Karim and Hawlader [82,83]. The energy balances for absorber plate, back insulation and working fluid of the above collector are given by the following Karim and Hawlader [83]:

$$\tau_g \alpha_p S + U_t(T_a - T_p) + h_1(T_f - T_p) + h_r(T_b - T_p) = 0 \tag{187}$$

$$U_b(T_a - T_b) + h_2(T_f - T_b) + h_r(T_b - T_p) = 0 \tag{188}$$

$$h_1(T_p - T_f) + h_2(T_b - T_f) = q_u \tag{189}$$

A series of experiments were conducted, data were recorded for different operating variables to determine the performance of v-groove solar air collectors. Experimental and analytical results have shown a good thermal performance of the v-groove collector. Satisfactory qualitative and quantitative agreement between experimental and analytical results was achieved.

An Internet based mathematical simulation has been conducted and developed by Bashria et al. [84,85] and Bashria et al. [86] to predict the thermal performance for different designs of solar air heaters with v-groove absorbers, single, double or triple glass covers.

Fig. 16a–c show the designs of v-groove solar air collector studied. A number of simplifying assumptions has been made to lay the foundation without obscuring the basic physical situation. These assumptions are as follows: (i) performance is steady state; (ii) There is no absorption of solar energy by a cover insofar as affects losses from the collector, (iii) Heat transfer fluid is considered a non-participating medium, (iv) The radiation coefficient between the two air duct surfaces is found by assuming a mean radiant temperature equal to the mean fluid temperature. (v) Loss through front and back are of the same temperature. The steady state energy equations yield the following equations:

In the single pass v-groove absorber:

$$\text{For the cover}: \quad U_t(T_g - T_a) = h_1(T_p - T_g) + h_r(T_p - T_g) \tag{190}$$

$$v\text{-groove absorber}: \quad \tau_g \alpha_p S = h_1(T_p - T_g) + h_r(T_p - T_g) + h_2(T_p - T_f) \tag{191}$$

$$\text{Fluid medium}: \quad h_2(T_p - T_f) + U_b(T_a - T_f) = \left(\frac{mC_f}{W}\right)\frac{dT_f}{dx} \tag{192}$$

In double pass double duct:

$$\text{For the cover}: \quad U_t(T_g - T_a) = h_1(T_p - T_g) + h_r(T_p - T_g) \tag{193}$$

$$v\text{-groove absorber}: \quad \tau_g \alpha_p S = h_2(T_p - T_{f1}) + h_1(T_p - T_g) + h_r(T_p - T_g) + h_3(T_p - T_{f2}) + h_{r2}(T_p - T_r) \tag{194}$$

$$\text{Fluid medium in the upper passage}: \quad h_2(T_p - T_{f1}) = \left(\frac{mC_f}{W}\right)\frac{dT_{f1}}{dx} \tag{195}$$

$$\text{Fluid medium in the lower duct}: \quad h_3(T_p - T_{f2}) + h_4(T_{f2} - T_r) = \left(\frac{mC_f}{W}\right)\frac{dT_{f2}}{dx} \tag{196}$$

$$\text{Bottom plate}: \quad U_b(T_r - T_a) = h_4(T_{f2} - T_r) + h_{r2}(T_p - T_r) \tag{197}$$

In double flow double duct packed:

$$\text{For the cover}: \quad U_t(T_g - T_a) = h_1(T_p - T_g) + h_r(T_p - T_g) \tag{198}$$

$$v\text{-groove absorber}: \quad \tau_g\alpha_p S = h_2(T_p - T_{f1}) + h_1(T_p - T_g) + h_r(T_p - T_g) + h_3(T_p - T_{f2}) + h_{r2}(T_p - T_{pr}) \tag{199}$$

$$\text{Fluid medium in the upper passage}: \quad h_2(T_p - T_{f1}) = \left(\frac{mC_{p1}}{W}\right)\frac{dT_{f1}}{dx} \tag{200}$$

$$\text{Fluid medium in the lower duct}: \quad h_3(T_p - T_{f2}) + h_4(T_{f2} - T_{pr}) + h_5(T_{f2} - T_r) = \left(\frac{mC_{p2}}{W}\right)\frac{dT_{f2}}{dx} \tag{201}$$

$$\text{Porous media}: \quad h_4(T_{pr} - T_{f2}) = h_{r2}(T_p - T_{pr}) + h_6(T_{pr} - T_r) \tag{202}$$

$$\text{Bottom plate}: \quad U_5(T_{f2} - T_r) + h_6(T_{pr} - T_r) = U_b(T_r - T_a) \tag{203}$$

The pressure drop through the channel in the air heater has been computed using the following expression [87]:

$$P = \left[f_0 + y\frac{D}{L}\right]\left(\frac{m^2}{\rho}\right)\left(\frac{L}{D}\right)^3 \tag{204}$$

where for $f_0 = 24/\text{Re}$, $y = 0.9$ for laminar flow ($\text{Re} < 2550$), $f_0 = 0.0094$, $y = 2.92\,Re^{-0.15}$ for transitional flow ($2550 < \text{Re} < 10^4$) and $f_0 = 0.059\,Re^{-0.2}$, $y = 0.73$ for turbulent flow ($10^4 < \text{Re} < 10^5$).

This mathematical model has been used recently by Bashria et al. [86] to find the effect of different parameters such as mass flow rate, flow channel depth and collector length on the system thermal performance and pressure drop through the collector (see Fig. 16a–c). The prototype internet program was developed to be used as a tool to support the design of solar air heaters used for drying. The results were validated by comparison the predicted output and the experimental results carried out by Karim and Hawlader [82]. A great correlation has occurred between the experimental and the predicted efficiencies. Also a good correlation has been found between the experimental and predicted efficiencies and outlet temperature, respectively.

Kabeel and Mecarik [50] have investigated v-groove air heater system with two covers and the flow passes over and under the absorber plate (Fig. 16d). By considering the energy balance for each part of the system in the steady state heat flow were written as the follow:

$$\text{For the upper glass cover}: \quad \alpha_{g1}S + h_{rg1g2}(T_{g2} - T_{g1}) + h_{cg1a1}(T_{a1} - T_{g1}) - h_w(T_{g1} - T_a) = 0 \tag{205}$$

$$\text{For the second glass cover}: \quad \tau_{g1}\alpha_{g2}S - h_{cg2a1}(T_{g2} - T_{a1}) - h_2(T_{f2} - T_{g2}) - h_{rg2g1}(T_{g2} - T_{g1}) + h_{rg2p}(T_p - T_{g2}) = 0 \tag{206}$$

$$\text{For the flow between the two glass covers}: \quad h_{g2a1}(T_{g2} - T_{a1}) - h_{g1a1}(T_{a1} - T_{g1}) = 0 \tag{207}$$

$$\text{For the absorber plate}: \quad \tau_{g1}\tau_{g2}\alpha_p S - Zh_{pf1}(T_p - T_{f1}) - Zh_{pf2}(T_p - T_{f2}) - h_{rpg2}(T_p - T_{g2}) - h_{rpb}(T_p - T_b) = 0 \tag{208}$$

$$\text{For Back plate}: \quad h_{rpb}(T_p - T_b) + h_{cbf1}(T_{f1} - T_b) - U_b(T_b - T_a) = 0 \tag{209}$$

Z is the ratio between the actual absorber area and the absorber area normal to the solar radiation following upon the collector. With this mathematical model taking into account the absorber shape factor, Kabeel and Mecarik [50] have outlined the effect of the change of the triangular angle θ on the pressure drop, on the heat transfer added to the flowing air and deduced the optimum angle of the v-groove.

2.15. Single pass solar air heater with packed

2.15.1. Type 1

The type 1 solar heater is shown in Fig. 17a. It consists of conventional configuration of Fig. 4 with the flow passage filled with packing. In the mathematical model proposed by Choudhury and Garg [88], energy balance equation of the cover is given by Eq. (36). For the absorber plate, packing and air flow and bottom plate, energy balance equations in the steady state were given by the follow:

$$\text{Absorber plate}: \quad \tau_g\alpha_p S = (h_{rgp} + h_{cgp})(T_p - T_g) + h_{rpp1}(T_p - T_{p1}) + h_{cpf}(T_p - T_f) \tag{210}$$

$$\text{Packing}: \quad h_{rpp1}(T_p - T_{p1}) = h_{cp1f}(T_{p1} - T_f) + h_{rp1b}(T_{p1} - T_b) \tag{211}$$

$$\text{Air flow}: \quad \frac{mC_f}{W}\frac{dT_f}{dx} = h_{cpf}(T_p - T_f) + h_{cp1f}(T_{p1} - T_f) + h_{cbf}(T_b - T_f) \tag{212}$$

$$\text{Bottom plate}: \quad h_{rp1b}(T_{p1} - T_b) = h_{cbf}(T_b - T_f) + U_b(T_b - T_a) \tag{213}$$

The boundary conditions for the above design are: $T_f(x = 0) = T_{fi}$, $T_f(x = L) = T_{fo}$. In this model, it was assumed that the heat transfer resulting from conduction in the packed flow channels is neglected due to point contacts between packing and the plates.

Recently, Paul and Saini [90] have used the mathematical model proposed by Choudhury and Garg [88] to outline the bed parameters in such a way that the solar energy collection systems deliver energy with minimum cost. A computer program in '*C*' language has been developed to obtain thermal efficiency and cost per unit energy delivered by packed bed solar air heater having wire mesh screens and pebbles as packing materials with different specifications. This program was validated by comparing some of the predicted values of thermal efficiency with experimental values obtained by Collier [92].

2.15.2. Type 2

It consists of two sheets of cover and the back plate; the passage between the inner cover and the back plate is provided with black-painted packing, which act as absorbers of solar radiation and transfer the heat to the air flowing through the packed channel (see Fig. 17b). This device has been investigated by Choudhury and Garg [88] and the energy balance written. Energy balance of the outlet cover, back plate and air flow were given by Eqs. (36), (212) and (213) respectively. For the inner cover and packing, the energy balances are as follows:

$$\text{For the inner cover}: \quad \tau_{g2}\alpha_{g1}S + h_{rp1g2}(T_{p1} - T_{p2}) = (h_{rg1g2} + h_{cg1g2})(T_{g2} - T_{g1}) + h_{cg2f}(T_{g2} - T_f) \tag{214}$$

$$\text{For the packing}: \quad \tau_{eff}\alpha_{p1}S = h_{cp1f}(T_{p1} + T_f) = h_{rp1g2}(T_{p1} + T_{p2}) + h_{rp1b}(T_{p1} + T_b) \tag{215}$$

This design has been used as a component of hybrid heating system [93,94]. To simulate the performance of this system, a transient analysis has been proposed by the authors where the above energy balance has been written for a rock bed solar air

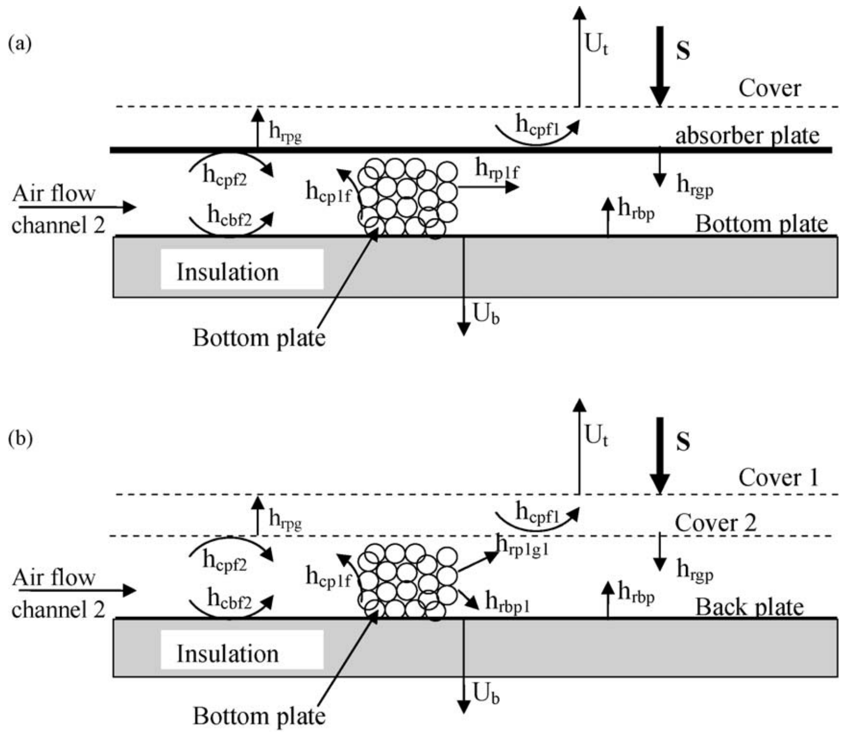


Fig. 17. (a) A schematic view of a single cover solar air heater (Choudhury and Garg [88]). (b) A schematic view of a single cover solar air heater (Choudhury et al. [88]).

heater.

$$M_{g1}C_{g1}\frac{dT_{g1}}{dt} = \alpha_{g1}S + h_{g1g2}(T_{g2} - T_{g1}) - h_{g1a}(T_{g1} - T_a) \quad (216)$$

$$M_{g2}C_{g2}\frac{dT_{g2}}{dt} = \tau_{g1}\alpha_{g2}S + h_{p1g2}(T_{p1} - T_{g2}) - h_{g2g1}(T_{g2} - T_{g1}) - h_{g2a}(T_{g2} - T_f) \quad (217)$$

$$M_{p1}C_{p1}\frac{dT_{p1}}{dt} = \tau_{g1}\tau_{g2}\alpha_{p1}S - h_{cp1f}(T_{p1} - T_f) - h_{rp1g2}(T_{p1} - T_{g2}) - h_{p1b}(T_{pi} - T_b) \quad (218)$$

$$M_fC_f\frac{dT_f}{dt} = -m_fC_f(T_o - T_{fi}) + h_{p1f}(T_{p1} - T_f) - h_{g2f}(T_{g2} - T_f) - h_{cbf}(T_b - T_f) \quad (219)$$

$$M_bC_b\frac{dT_b}{dt} = h_{p1b}(T_{p1} - T_b) - h_{cbf}(T_b - T_f) - U_b(T_b - T_a) \quad (220)$$

The results have shown that the hybrid air-to-water heating system performs much better when coupled with a rock bed air heater than when coupled to a conventional empty channel air-heating collector.

2.16. Double-pass solar air heater with packed

The schematic diagrams of the double-pass solar air heater with packed bed are shown in Fig. 18. The different heat transfer mechanisms in terms of the various heat transfer coefficients are also shown. The air was firstly forced through the packed bed existing in the upper channel (Fig. 18a), formed between the lower cover and the absorber plate, and is then re-circulated to flow in the opposite direction through the lower channel, formed between the absorber and back plates. Ramadan et al. [96] have investigated heat transfer in this solar heater. The mathematical model has been developed taking account of the following assumptions: (i) the air heater operates under steady state conditions. However, the model remains transient due to the time dependence of solar radiation intensity and ambient temperature. (ii) The heat capacities of the glass covers, absorber and back plates and insulation were negligible. (iii) The temperature of the flowing air was varied only in the direction of flow. (iv) The thermo physical properties of the flowing air were assumed to vary linearly with temperature (see [7]). (v) There was no temperature gradient across the thickness of the covers, the absorber and the back plates. On the basis of the above assumptions, the energy balance equations for the different components of the air heater were written as follows:

$$\text{Cover 2}: \quad A_g\alpha_gS = A_g(h_{rg1g2} + h_{cg1g2})(T_{g2} - T_{g1}) + h_wA_g(T_{g2} - T_a) + A_gh_{rg2sky}(T_{g2} - T_{sky}) \quad (221)$$

$$\text{Cover 1}: \quad A_g\alpha_g\tau_gS = A_g(h_{rg1g2} + h_{cg1g2})(T_{g1} - T_{g2}) - h_{rp1g1}A_g(T_{p1} - T_{g1}) - A_gh_{cg1f1}(T_{f1} - T_{g1}) \quad (222)$$

$$\text{Air flow in upper channel}: \quad Wh_{pf1}(T_p - T_{f1}) + Wh_{cp1f1}(T_{p1} - T_{f1}) = m_{f1}C_f\frac{dT_{f1}}{dx} + Wh_{cg1f1}(T_{f1} - T_{g1}) + WU_s(T_{f1} - T_a) \quad (223)$$

$$\text{Absorber plate}: \quad A_ph_{rp1p}(T_{p1} - T_p) = A_ph_{pf1}(T_p - T_{f1}) + A_ph_{pf2}(T_p - T_{f2}) + A_ph_{rpb}(T_p - T_b) \quad (224)$$

$$\text{Air flow in lower channel}: \quad Wh_{pf2}(T_p - T_{f2}) + Wh_{f2b}(T_b - T_{f2}) = m_{f2}C_{f2}\frac{dT_{f2}}{dx} + WU_s(T_{f2} - T_a) \quad (225)$$

$$\text{Back plate}: \quad A_bh_{bf2}(T_{f2} - T_b) + A_bh_{rpb}(T_p - T_b) = A_bU_b(T_b - T_a) \quad (226)$$

The various heat transfer coefficients given in the above equations were calculated using the correlation given in the literature [7]. A suitable computer program was prepared, for the solution of the energy balance equations for different elements of

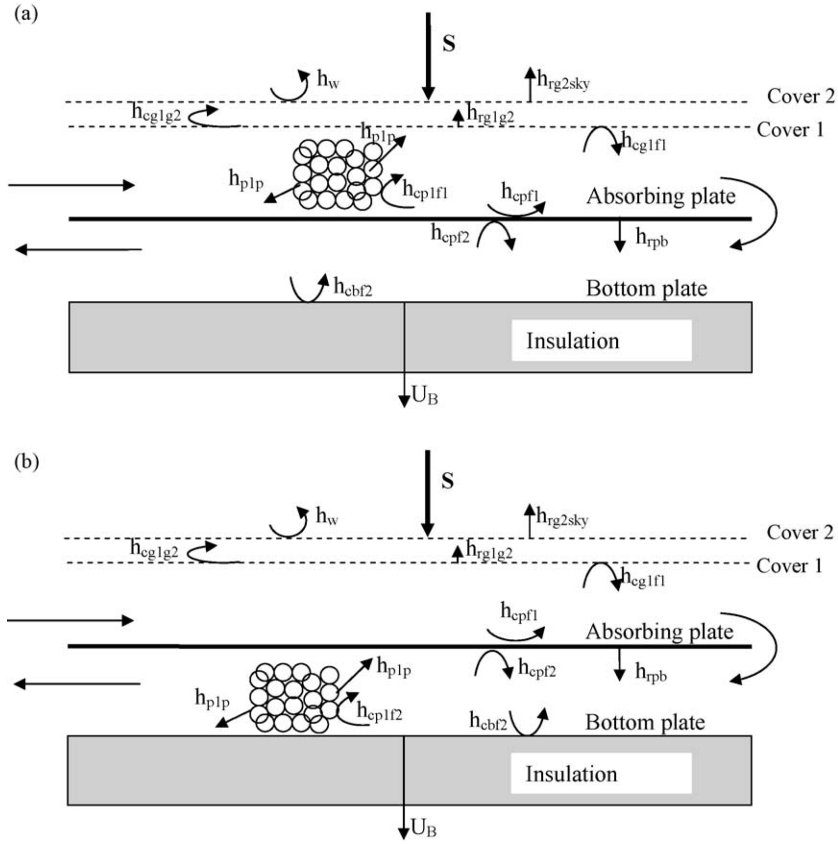


Fig. 18. (a) Schematic view of energy-flow of double-pass type solar air heater with recycle (see Ramadan et al. [96]). (b) Schematic view of energy-flow of double-pass type solar air heater with recycle (see El-Sebaii et al. [99]).

the solar air heater. It was inferred that for increasing the outlet temperature of the flowing air after sunset, it was advisable to use the packed bed materials with higher masses and therefore with low porosities. It was recommended to operate the system with packed bed with values of the mass flow rate equal 0.05 kg/s or lower to have a lower pressure drop across the system. This mathematical model has been validated by comparisons between experimental and theoretical results showing that good agreement was achieved.

El-Sebaii et al. [99] have proposed an investigation of heat transfer on a double-pass solar air heater in which the air was firstly forced through the upper channel, formed between the lower cover and the absorber plate, and then re-circulated to flow in the opposite direction through the packed bed that exists in the lower channel, formed between the absorber and back plates (Fig. 18b). With the above assumptions, El-Sebaii et al. [99] have written the energy balance equations for the system. For cover 2, energy balance equation is given by Eq. (221). For cover 1, air flowing in upper channel, absorber plate, air flowing in the lower channel and back plate may be written as follows, respectively:

$$A_g\alpha_g\tau_g S - A_g(h_{rg1g2} + h_{cg1g2})(T_{g1} - T_{g2}) = -h_{rp1g1}A_g(T_{p1} - T_{g1}) - A_g h_{cg1f1}(T_{f1} - T_{g1}) \quad (227)$$

$$\text{Air flow in upper channel}: \quad Wh_{pf1}(T_p - T_{f1}) + Wh_{cp1f1}(T_{p1} - T_{f1}) = m_{f1}C_f\frac{dT_{f1}}{dx} + Wh_{cg1f1}(T_{f1} - T_{g1}) + WU_s(T_{f1} - T_a) \quad (228)$$

$$\text{Absorber plate}: \quad \alpha_p\tau_g^2 A_p S = A_p h_{cpf1}(T_p - T_{f1}) + A_p h_{cpf2}(T_p - T_{f2}) + A_p h_{rpg1}(T_p - T_{g1}) + A_p h_{rpp1}(T_p - T_{p1}) \quad (229)$$

$$\text{Air flow in lower channel}: \quad Wh_{pf2}(T_p - T_{f2}) + Wh_{cp1f2}(T_{p1} - T_{f2}) = m_{f2}C_{f2}\frac{dT_{f2}}{dx} + WU_s(T_{f2} - T_a) + Wh_{bf2}(T_{f2} - T_b) \quad (230)$$

$$\text{Back plate}: \quad A_b h_{bf2}(T_{f2} - T_b) + A_b h_{rp1b}(T_{p1} - T_b) = A_b U_b(T_b - T_a) \quad (231)$$

The various heat transfer coefficients given in the above equations were calculated using the correlation given in literature [97,98]. The program developed by Ramadan et al. [96] was used. On the basis of the obtained results for the solar air heater, it had been concluded that (i) to enhance the convective heat transfer coefficients to the flowing air, as well as the heater efficiency, it was advisable to operate the system with the packed bed above the absorber plate with low porosity and relatively high mass flow rates of air. (ii) It was better to use gravel instead of limestone as a packed bed above the absorber plate. (iii) It was recommended to operate the system with and without the packed bed with values of the mass flow rate equal to 0.05 kg/s or lower to have a lower pressure drop across the system, and therefore, reasonably high thermo hydraulic efficiency. (iv) It was better to use materials with high thermal conductivity, such as iron scraps, as packed beds above the absorber plate if a higher outlet temperature of air is required during sunshine hours. Gravel as a packed bed above the

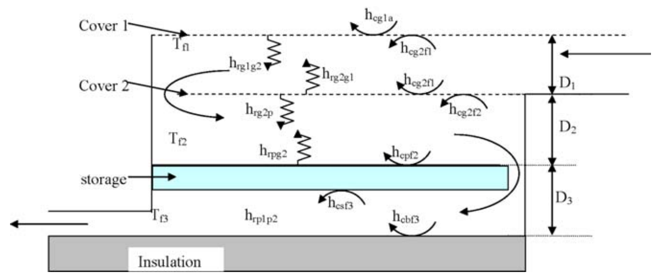


Fig. 19. Three pass two covers air heater with in-built thermal storage (Jain and Jain [100], Jain [101]).

absorber plate during low intensity solar radiation periods was recommended.

2.17. Multi-pass solar air heater with in-built thermal storage

Recently, Jain and Jain [100] and Jain [101], studied an indirect solar crop dryer coupled with the solar air heater, investigated the heat transfer in the multi-pass solar air heater with in-build thermal storage. The schematic diagram is shown in Fig. 19. In this model, the solar radiation transmits from the glass covers and is absorbed by the absorber plate. The air flows in between the covers, above the absorber plate and below the storage material, where it is heated along the path. Jain and Jain [100] and Jain [101] have written the energy balance equations for this design on the base of the following assumptions (i) the heat capacities of the air, covers, absorber plate and insulation were negligible; (ii) there was no temperature gradient along the thickness of cover; (iii) storage material has an average temperature (T_s) at a time t, (iv) there was no stratification existing perpendicular to the air flow in ducts, (v) the system was perfectly insulated and there was no air leakage. Based on these assumptions, energy balance equations on the double-cover multi-pass flat plate collector with in-built thermal storage were given as follows:

For the first cover: $$\alpha_{g1}A_{g1}S_{eff} + h_{rg2g1}A_{g1}(T_{g2} - T_{g1}) = h_{cg1f1}A_{g1}(T_{g1} - T_{f1}) + h_{cg1a}A_{g1}(T_{g1} - T_a) + h_{rg1sky}A_{g1}(T_{g1} - T_{sky}) \quad (232)$$

where $T_{sky} = T_a - 6$ (see [102]):

For the second cover: $$\alpha_{g2}\tau_{g1}A_{g2}S_{eff} + h_{rpg2}A_{g2}(T_p - T_{g2}) + h_{cf1g2}A_{g2}(T_{f1} - T_{g2}) = h_{rg2g1}A_{g2}(T_{g2} - T_{g1}) + h_{cg2f2}A_{g2}(T_{g2} - T_{f2}) \quad (233)$$

For the absorber plate: $$\alpha_p\tau_{g1}\tau_{g2}A_{g2}S_{eff} = h_{rpg2}A_p(T_p - T_{g2}) + h_{cpf2}A_p(T_p - T_{f2}) + h_{cps}A_p(T_p - T_s) \quad (234)$$

For air flow in the first channel: $$Wh_{cg1f1}(T_{g1} - T_{f1}) = mC_f\frac{dT_{f1}}{dx} + Wh_{cf1g2}(T_{f1} - T_{g2}) \quad (235)$$

For air flow in the second channel: $$Wh_{cg2f2}(T_{g2} - T_{f2}) = mC_f\frac{dT_{f2}}{dx} + Wh_{cpf2}(T_{f1} - T_{g2}) \quad (236)$$

For air flow in the third channel: $$Wh_{csf3}(T_s - T_{f3}) = mC_f\frac{dT_{f2}}{dx} + WU_b(T_{f3} - T_a) \quad (237)$$

For the storage material: $$h_{cps}(T_p - T_s)A_p = M_sC_s\frac{dT_s}{dt} + h_{csf3}(T_s - T_{f3})A_p \quad (238)$$

The convective heat transfer coefficients from the plate to cover, parallel to each other and inclined at the angle β to horizontal has been expressed given in literature [7,27] and in the appendix. Jain and Jain [100] have computed solar intensity on the inclined surface by using the method given by Lui and Jordan [103]. A computer program was prepared to solve the above set of equations. The performance evaluation of a tilted multi-pass solar air heater with in-built thermal storage has been carried out for deep-bed drying applications. The thermal energy storage also affect during the off-sunshine hours is very pertinent for crop drying applications. With the above mathematical model, Jain [101] has shown that it is useful to evaluate the thermal performance of a flat plate solar air heater for the crop drying in multiple trays.

2.18. Matrix (porous) solar air heater

The porous or matrix type solar air heaters are shown in Fig. 20a and b. It consists of single glazing at the top, matrix, back metallic plate and insulation. In the first design (Fig. 20a) the air flow is upward through the matrix and in the second design (Fig. 20b), it is flow downward through the matrix. These models have been investigated by Sharma et al. [98] and Sharma et al. [104]. Sharma et al. [98] analyzed the various energy exchanges inside the porous bed. The energy balance equations were described by the following equations for air flowing upward:

$$M_bC_b\frac{\partial T_b}{\partial t} = k_b\frac{\partial^2 T_b}{\partial y^2} - h_{fv}(T_b - T_f) + \alpha a S\exp(-ay) \quad (239)$$

$$M_fC_f\frac{\partial T_f}{\partial t} = GC_f\frac{\partial^2 T_f}{\partial y^2} - h_{fv}(T_b - T_f) \quad (240)$$

The corresponding relations for air flowing downward can be obtained from the above equation by changing the sign of G. The above equations were solved explicitly. The results were showed that such types of solar air heater have the tendency to maintain a constant efficiency throughout the operation. The experiment was also carried out. A good agreement of the theory with experimental observations almost confirms that the model can be used to predict the performance of the porous solar air heaters.

A transient model for a matrix air heater having a single glazing at the top and a thin metallic plate backed by an insulator at the bottom was presented by Sharma et al. [104]. The mathematical model used was similar to the one obtained by Sharma et al. [98] in

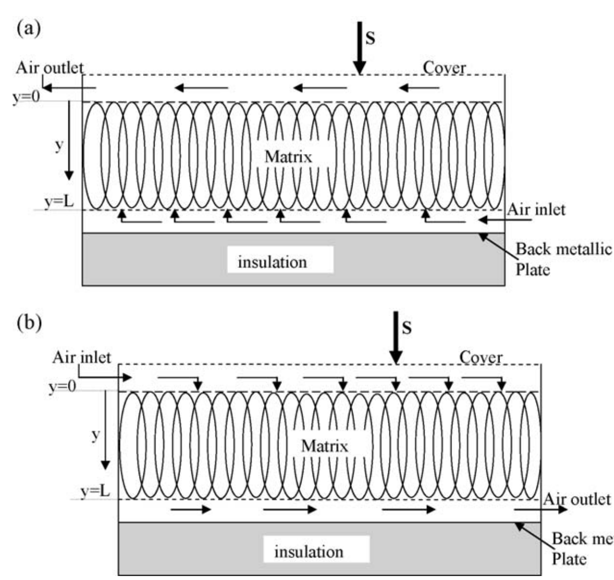


Fig. 20. (a) Matrix air heater (air flow upward) (Sharma et al. [98]). (b) Matrix air heater (air flow downward) (Sharma et al. [98,104]).

the air flow downward air heater. In this model solar insulation and ambient temperature were represented by Fourier series in time with y dependent Fourier coefficients. The experimental results for a varying inlet air flow rate were analyzed and the rating parameters were included. From the results, it was observed that the matrix air heater concept shows promise for collection enhancement of energy at a cost lower than most of other conventional solar air heaters.

3. Conclusion

Many mathematical approaches have been developed for simulating the performance of solar air heaters. In this work, a review is given of the present state of mathematical modeling based on the energy analysis.

The models on energy analysis are usually expressed in relatively simple equations and are based on the steady state of the system. Certain assumptions used in the mathematical form appear to be too ideal. However these models are limited by the heat transfer efficiency between the absorber and the fluid. Since heat transfer augmentation usually increases friction, optimum parameters, such as mass flow and collector geometry, have to be determined.

Model validation is a key step in model development since it offers the possibility of comparing computed results with actual system behavior. Experiments and/or comparison with known analytical, or previous numerical results are mostly used to validate the mathematical model. Good agreement is generally observed and the computed trends are also compatible with those reported for experimental observations. However, there appears to be a lack of agreement among authors in several areas and furthermore, there are still some key deficiencies that can only be addressed through continued enhancement of the existing modeling techniques. As such, there exists a large body of work to predict several features of the process.

Future work should be directed towards a more comprehensive description of heat transfer phenomena, which would involve the generation of more information in the exergy analysis of the solar air heaters.

Acknowledgments

This work was done within the framework of the Associateship Scheme of ICTP. Financial support from the Swedish International Development Cooperation Agency is also acknowledged.

Appendix A

The convective heat transfer coefficient h_w for air flowing over the outside surface of the cover depends primarily on the wind velocity V. MacAdams [19] obtained the experimental result:

$$h_w = 5.7 + 3.8\ V \qquad (0 \le V \le 5\ \text{m/s}) \tag{A1}$$

where the units of h_w and V are W/m^2 C and m/s, respectively. If the unit of h_w is changed to Kj/h m^2 K, the above equation becomes:

$$h_w = 4.9 + 3.2\,V \tag{A2}$$

This coefficient has also been given by Watmuff, Charters and Proctor [109] as:

$$h_w = 2.8 + 3.0\,V \qquad (0 \le V \le 7\ \text{m/s}) \tag{A3}$$

An empirical equation for U_T was developed by Klein [67] following the basic procedure of Hottel and Woertz [68]. For a horizontal collector with two glass covers U_T is given by the relationship:

$$U_T = U_{T1} + U_{T2} \tag{A4}$$

With

$$U_{T1} = \left\{ \frac{2(T_{pm}/520)}{[(T_{pm}/T_{sky})/2 + (1 + 0.089)h_w - 0.1166 h_w \varepsilon_p (1 + 0.7866 \times 2)]^{0.43(1-100/T_{pm})}} \right\}^{-1}$$

$$U_{T2} = \frac{\sigma(T_{pm} + T_{sky})(T_{pm}^2 + T_{sky}^2)}{(\varepsilon_p + 2 \times 0.00591\,h_w)^{-1} + [2 \times 2 + (1 + 0.089\,h_w - 0.1166\,h_w \varepsilon_p)(1 + 0.07866 \times 2) - 1 + 0.133\,\varepsilon_p]/\varepsilon_p - 2}$$

References

[1] Chandra R, Sodha MS. Testing procedures for solar air heaters: a review. Energy Conversion and Management 1991;32(1):11–33.
[2] Shaobo H, Zeng D, Ye S, Zhang H. Exergy analysis of the solar multi-effect humidification-dehumidification desalination process. Desalination 2007; 203:403–9.
[3] Ekechukwu OV, Norton B. Review of solar-energy drying systems III: low temperature air-heating solar collectors for crop drying applications. Energy Conversion and Management 1999;40:657–67.
[4] Choudhury C, Chauhan PM, Garg HP. Design curves for conventional solar air heaters. Renewable energy 1995;6(7):739–49.
[5] Duffie JA, Beckmann WA. Solar engineering of thermal processes. New York: Wiley; 1980.
[6] Tan HM, Charters WS. Effect of thermal entrance region on turbulent forced convective heat transfer for an asymmetrically heater rectangular duct with uniform heat flux. Solar Energy 1969;12:513.
[7] Ong KS. Thermal performance of solar air heaters: mathematical model and solution procedure. Solar Energy 1995;55(2):93–109.
[8] Njomo D. Unglazed selective absorber solar air collector: heat exchange analysis. Heat Mass Transfer Wärme 2000;36:313–7.
[9] Njomo D, Daguenet M. Sensitivity analysis of thermal performances of flat plate solar air heaters. Heat Mass Transfer 2006;42:1065–81.
[10] Sparrow EM, Ramsey JW, Mass EA. Effect of finite width on heat transfer and fluid flow about an inclined rectangular plate. Journal of Heat Transfer—Transactions of the ASME 1979;101:199–204.
[11] Mercer WE, Pearce WM, Hichcock JE. Laminar forced convection in the entrance region between parallel flat plates. Journal of Heat Transfer—Transactions of the ASME 1967;89:251–7.
[12] Clark D. Passive/hybrid comfort cooling by thermal radiation. In: Passive/hybrid cooling conference, Miami; 1981.
[13] Garg HP, Chandra R, Rani U. Transient analysis of solar air heaters using finite differences technique. Energy Research 1981;5:243–52.
[14] Njomo D. Modelling the heat exchanges in a solar air heater with a cover patially transparent to infrared radiation. Energy Conversion and Management 1991;31(5):495–503.
[15] Mohamad AA. High efficiency solar air heater. Solar Energy 1997;60(2): 71–6.
[16] Hegazy AA. Performance of the flat solar air heaters with optimum channel geometry for constant/variable flow operation. Energy Conversion and Management 2000;41:401–17.
[17] Paisarn N, Kongtragool B. Theoretical study on heat transfer characteristics and performance of the flat-plate solar air heaters. International Communications in Heat and Mass Transfer 2003;30(8):1125–36.
[18] Zhai XQ, Dai YJ, Wang RZ. Comparison of heating and natural ventilation in a solar house induced by two roof solar collectors. Applied Thermal Engineering 2005;25:741–57.
[19] McAdams WH. Heat transmission. New York: McGraw-Hill; 1954.

[20] Kreith F, Kreider JF. Principles of solar engineering. New York: McGraw-Hill; 1978.
[21] Heaton HS, Reynolds WC, Kays WM. Heat transfer in annular passages. Simultaneous development of velocity and temperature fields in laminar flow. International Journal of Heat and Mass Transfer 1964;7:763–81.
[22] Hausen H. Darstellung des warmenberganges in rohren durch verallgemeinerte potenzbeiziehungen. VDIZ 1943;4:91–8.
[23] Tan HM, Charters WS. an experimental investigation of forced-convective heat transfer for fully-developed turbulent flow in a rectangular duct with asymmetric heating. Solar Energy 1970;13:121–5.
[24] Niles PW, Carnegie EJ, Pohl JG, Cherne JM. Design and performance of an air collector for industrial crop dehydration. Solar Energy 1979;20(1):19–23.
[25] Yeh HM, Lin TC. The effect of collector aspect ratio on the collector efficiency of flat-plate solar air heaters. Energy 1995;20(10):1041–7.
[26] Hegazy AA. Thermohydraulic performance of heating solar collectors with variable width, flat absorber plates. Energy Conversion and Management 2000;41:1361–78.
[27] Aboul-Enein S, El-Sebaii AA, Ramadan MRI, El-Gohary HG. Parametric study of a solar air heater with and without thermal storage for solar drying applications. Renewable Energy 2000;21:505–22.
[28] Hollands KGT, Unny TE, Raithby GR, Konicek L. Free convective heat transfer across inclined air layers. Journal of Heat Transfer—Transactions of the ASME 1976;98(2):189–93.
[29] Siegel R, Howel JR. Thermal radiation heat transfer. Washington: Hemisphere Publishing Corporation; 1981.
[30] Njomo D. Techno-economic analysis of a plastic cover solar air heater. Energy Conversion and Management 1995;36(10):1023–9.
[31] Njomo D. Etude théorique du comportement thermique d'un capteur solaire plan a air a couverture combine plastique vitre. Revue Generale de Thermique 1998;37:973–80.
[32] Garg HP, Datta G, Bhargava K. Some studies on the flow passage dimension for solar air testing collector. Energy Conversion and Management 1984;24(3): 181–4.
[33] Choudhury C, Chauhan PM, Garg HP. Performance and cost analysis of two-pass solar air heaters. Heat Recovery Systems & CHP 1995;15(8):755–73.
[34] Al-Kamil MT, Al-Ghareeb AA. Effect of thermal radiation inside solar air heaters. Energy Conversion and Management 1997;38(14):1451–8.
[35] Jannot Y, Coulibaly Y. Radiative heat transfer in a solar air heater covered with a plastic film. Solar Energy 1997;60(1):35–40.
[36] Hegazy AA. Optimum channel geometry for solar air heaters of conventional design and constant flow operation. Energy Conversion and Management 1999;40:757–74.
[37] Hollands KGT, Shewen EC. Proc. Int. Sol. Energy Soc. Congr., SUN II, Silver Jubilee Congr, Atlanta, GA; 1979.
[38] Biehl FA. Test results and analysis of a convective loop solar air collector. In. Proceedings of 6th National Passive Solar Conference Portland, Oregon (cited by Alfeld K et al., 1988); 1981.
[39] Jha RK, Choudhury C, Garg HP, Zaidi ZH. Performance prediction of a solar heater house. Energy Conversion and Management 1992;33(4):263–73.
[40] Ucar A, Inalli M. Thermal and exergy analysis of solar air collectors with passive augmentation technique. International Communication in Heat and Mass Transfer 2006;33:1281–90.
[41] Wong HY, Handbook of essential formula and data on heat transfer for engineers, London; 1977.
[42] Siedel EN, Tate GE. Heat transfer and pressure drop of liquids in tubes. Industrial and Engineering Chemistry 1936;28:1429–35.
[43] Forson FK, Nazha MAA, et Rajakaruna H. Experimental and simulation studies on a single pass, double duct solar air heater. Energy Conversion and Management 2003;44:1209–27.
[44] Achenbach PR, Cole SD. Performance of fourteen masonry chimneys under steady state conditions. Transactions of the ASHVE 1949;55:129–54.
[45] Yeh Ho-Ming, Chii-Dong Ho, Jun-Ze Hou. The improvement of collector efficiency in solar air heaters by simultaneously air flow over and under the absorbing plate. Energy 1999;24:857–71.
[46] Kays WM. Convective heat and mass transfer. New York: McGraw-Hill; 1980.
[47] Yeh Ho-Ming, Ho Chii-Dong, Hou Jun-Ze. Collector efficiency of double-flow solar air heaters with fin attached. Energy 2002;27:715–27.
[48] Al-Nimr MA, Damseh RA. Dynamic behaviour of baffled solar air heaters. Renewable Energy 1998;13(2):153–63.
[49] Matrawy KK. Theoretical analysis for an air heater with a box-type absorber. Solar Energy 1998;63(3):191–8.
[50] Kabeel AE, Mecarik KK. Shape optimization for absorber plates of solar air collector. Renewable Energy 1998;13(1):121–31.
[51] Ammari HD. A mathematical model of thermal performance of a solar air heater with slats. Renewable Energy 2003;28:1597–615.
[52] Duffie JA, Beckmann WA. Solar engineering of thermal processes, 2nd ed., Toronto: John Wiley & Sons, Inc.; 1991. p. 949.
[53] Nusselt W. Der warmeaustatsch zwischen wand und wasser im rohr. Forshung auf dem Gebiete des Ingenieurwesens 1931;2:309.
[54] Swinbank WC. Long-wave radiation from clear skies. QJR Meteorological Society 1963;89–339.
[55] Satcunanathan, Deonarine. A two-pass solar air heater. Solar Energy 1973;15:41.
[56] Caouris Y, et al. A novel solar collector. Solar Energy 1978;21:157.
[57] Wijeysundera NE, Lee Lee AH, Tjioe LK. Thermal performance study of two-pass solar air heaters. Solar Energy 1982;28(5):363–70.
[58] Wijeysundera NE. A net radiation method for the transmittance and absorptivity of series of parallel regions. Solar Energy 1975;17:75.
[59] Verma Ratna, Chandra Ram, Garg HP. Optimization of solar air heaters of different designs. Renewable Energy 1992;2(4/5):521–31.
[60] Choudhury S C., Garg HP. Comparative performance of Coriander dryer coupled to solar air heater and solar air-heater-cum-rock bed storage. Applied Thermal Engineering 1996;16(6):475–86.
[61] Hollands KGT, Shewen EC. Optimization of flow passage geometry for air-handling plate type solar collectors. Journal of Solar Energy Engineering 1981;103:323–30.
[62] Hirunlabh J, Kongduang W, Namprakai P, Khedari J. study of natural ventilation of houses by a solar wall under tropical climate. Renewable Energy 1999;18:109–19.
[63] Yamali Cemil, Ismail Solmus. Theoretical investigation of humidification-deshumidification desalination system configured by a double-pass flat solar air heater. Desalination 2007;205:163–77.
[64] Incropera FP, Dewitt DP. Fundamentals of heat and mass transfer, 3rd ed., Wiley; 1990.
[65] Yeh Ho-Ming, Chii-Dong Ho, Wen-Song Sheu. Double-pass heat or mass transfer through a parallel-plate channel with recycle. International Journal of Heat and Mass Transfer 2000;43:487–91.
[66] Ho CD, Yeh HM, Wang RC. Heat-transfer enhancement in double-pass flat-plate solar air heaters with recycle. Energy 2005;30:2796–817.
[67] Klein SA. Calculation of flat-plate loss coefficients. Solar Energy 1975;17: 79–80.
[68] Hottel HC, Woertz BB. Performance of flat plate solar heat collectors. Transactions of the ASME 1942;64:91–104.
[69] Paisarn N. Effect of porous media on the performance of double-pass flat plate solar air heater. International Communication of Heat and Mass Transfer 2005;32. N 3.
[70] Sopain K, Supranto, Daud WRW, Othman MY, Yatim B. Renewable Energy 1999;18:557.
[71] Paisarn N. On the performance and entropy generation of the double-pass solar air heater with longitudinal fins. Renewable Energy 2005;30(9):1345–57.
[72] Chandra R, Singh NP, Sodha MS. Thermal performance of triple-pass solar air collector. Energy Conversion and Management 1990;30(1):41–8.
[73] Sisson LE, Pitts DR. Elements of transport phenomena. New York: McGraw-Hill; 1972. pp. 681–686.
[74] Ezeike GOI. Energy in Agriculture 1986;5:1–20.
[75] Choudhury C, Chauhan PM, Garg HP, Garg SN. Cost-benefit ratio of triple pass solar air heaters. Energy Conversion and Management 1996;37(1):95–116.
[76] Ho CD, Yeh HM, Hsieh SM. Improvement in device performance of multi-pass flat-plate solar air heaters with external recycle. Renewable Energy 2005;30:1601–21.
[77] Pramuang S, Exell RHB. Transient test of a solar air heater with a compound parabolic concentrator. Renewable Energy 2005;30:715–28.
[78] Tchinda R. Thermal behaviour of solar air heater with compound parabolic concentrator. Energy Conversion and Management 2007. doi: 10.1016/j.enconman.2007.08.004.
[79] Hsieh CK. Thermal analysis of CPC collectors. Solar Energy 1981;27:19–27.
[80] Rabl A, Goodman NB, Winston R. Practical design considerations for CPC solar collectors. Solar Energy 1979;22:373–81.
[81] Brodkey RS, Hershey HC. Transport phenomena. McGraw-Hill Book Company; 1988.
[82] Karim Azharul Md, Hawlader MNA. Development of solar air collectors for drying applications. Energy Conversion and Management 2004;45:329–44.
[83] Azharul Md K, Hawlader MNA. Performance evaluation of v-groove solar air collector for drying applications. Applied Thermal Engineering 2006;26: 121–30.
[84] Bashria AA, Adam NM, SAPUAN SM, Daud M, Omar H, Megat HM, Abas F. Prediction of thermal performance of solar air heaters by internet-based simulation. Proceedings of the Institution of Mechanical Engineers Part A Journal of Power and Energy 2004;218:579–87.
[85] Bashria AA, Yousef, Adam NM, Daud M, Omar H, Ahmed MHM, Musa Elradi A. Expert system based prediction of the performance of solar air collectors in Malaysia. JEE 2004;3:91–101.
[86] Bashria AA, Yousef, Adam NM. Performance analysis for v-groove absorber. Suramaree Journal of Science and Technology 2007;14(1):39–52.
[87] Verma R, Chandra R, Garg HP. Technical note-optimization of solar air heaters of different designs. Renewable Energy 1992;2(4/5):521–31.
[88] Choudhury C, Garg HP. Performance of air-heating collectors with packed airflow passage. Solar Energy 1993;30(3):205–21.
[89] Paul B, Saini JS. Optimization of bed parameters for packed bed solar energy collection system. Renewable Energy 2004;29:1863–76.
[90] Dixon AG, Cresswell DL. Theoretical prediction of effective heat transfer parameters in packed beds. American Institute of Chemical Engineers 1979;25:663.
[91] Varshney L, Saini JS. Heat transfer and friction factor correlations for rectangular solar air heater duct with wire mesh screen matrices. Solar Energy 1998;62(4):255–62.
[92] Collier RK. The characterization of crushed glass as a transpired air heating solar collector material. In: Proceedings of the International Solar Energy Society; 1979. p. 264–8.
[93] Choudhury C, Garg HP. Performance calculations for closed-loop ai-t-heater solar hybrid heating systems with and without a rock bed in the solar air heater. Renewable Energy 1993;3(8):897–905.

[94] Choudhury C, Garg HP. Thermal performance of a solar hybrid domestic hot water system. Energy 1992;17(7):703–11.
[95] Duffie JA, Beckmann WA. Solar energy thermal processes. New York: Wiley; 1974.
[96] Ramadan MRI, El-Sebaii AA, Aboul-Enein S, El-Bialy E. Thermal performance of a packed bed double-pass solar air heater. Energy 2007;32:1524–35.
[97] Garg HP. Advances in solar energy technology. Dordrecht: Reidel publishing Company; 1987.
[98] Sharma VK, Sharma Sanjay, Mahajan RB, Garg HP. Evaluation of a matrix solar air heater. Energy Conversion and Management 1990;30(1):1–8.
[99] El-Sebaii AA, Abou-Enein S, Ramadan MRI, El-Bialy E. Year round performance of double pass solar air heater with packed bed. Energy Conversion and management 2007.
[100] Jain D, Jain RK. Performance evaluation of an inclined multi-pass solar heater with in-built thermal storage on deep-bed drying application. Journal of Food Engineering 2004;65:497–509.
[101] Jain D. Modelling the system performance of multi-tray crop drying using an inclined multi-pass solar air heater with in-built thermal storage. Journal of Food Engineering 2005;71:44–54.
[102] Whillier A. Design factors influencing solar collectors, low temperature engineering application of solar energy. New York: American Society of Heating, Refrigerating and Air conditioning Engineers, Inc.; 1967.
[103] Lui BYH, Jordan RC. Daily insulation on surfaces tilted towards equator. ASHRAE Journal 1962;3(10):53.
[104] Sharma VK, Rizzi G, Garg HP. Design and development of a matrix type solar air heater. Energy Conversion and Management 1991;31(4):379–88.